Weierstraß-Institut
für Angewandte Analysis und Stochastik
Leibniz-Institut im Forschungsverbund Berlin e. V.

Preprint ISSN 0946 – 8633

A diffuse interface model for quasi–incompressible flows: Sharp interface limits and numerics

Gonca Aki[1], Johannes Daube[2], Wolfgang Dreyer[1], Jan Giesselmann[3],

Mirko Kränkel[2], Christiane Kraus[1]

submitted: January 20, 2012

[1]Weierstrass Institute
Mohrenstr. 39
10117 Berlin
Germany
E-Mail: Gonca.Aki@wias-berlin.de
Wolfgang.Dreyer@wias-berlin.de
Christiane.Kraus@wias-berlin.de

[2]Department of Mathematics
University of Freiburg
Eckerstr. 1
Hermann-Herder-Str. 3a
79104 Freiburg
Germany
E-Mail: hannes@mathematik.uni-freiburg.de
kraenkel@mathematik.uni-freiburg.de

[3]ACMAC
University of Crete
Knossos Avenue
71409 Iraklio–Crete
Greece
E-Mail: jan.giesselmann@acmac.uoc.gr

No. 1680
Berlin 2012

2010 *Mathematics Subject Classification.* 35C20, 35R35.

Key words and phrases. Liquid vapor flow, phase transition, asymptotic analysis, sharp interface limit, free boundary problem

GA, WD and CK would like to thank the German Research Foundation (DFG) for financial support of the project "Modeling and sharp interface limits of local and non-local generalized Navier–Stokes–Korteweg Systems". JD and MK would like to thank the German Research Foundation (DFG) for financial support of the project within the research initiative "Micro–Macro Modeling and Simulation of Liquid–Vapour Flows". JG would like to thank the German Research Foundation (DFG) for financial support of the project within the Cluster of Excellence in Simulation Technology (EXC 310/1) at the University of Stuttgart.

Edited by
Weierstraß-Institut für Angewandte Analysis und Stochastik (WIAS)
Leibniz-Institut im Forschungsverbund Berlin e. V.
Mohrenstraße 39
10117 Berlin
Germany

Fax: +49 30 2044975
E-Mail: preprint@wias-berlin.de
World Wide Web: http://www.wias-berlin.de/

Abstract

In this contribution, we investigate a diffuse interface model for quasi–incompressible flows. We determine corresponding sharp interface limits of two different scalings. The sharp interface limit is deduced by matched asymptotic expansions of the fields in powers of the interface. In particular, we study solutions of the derived system of inner equations and discuss the results within the general setting of jump conditions for sharp interface models. Furthermore, we treat, as a subproblem, the convective Cahn–Hilliard equation numerically by a Local Discontinuous Galerkin scheme.

1. Introduction

We are interested in the modeling and numerical simulation of multiphase and multicomponent flows. We use a mixture approach, in which the constituents are either different substances or different phases of the same substance. In the description of multiphase and multicomponent flows, there are two different classes of models. Classically, one uses so called "sharp interface" models, where the interface between the substances or phases is described as a hypersurface. In the bulk domains separated by the interface, the fields – density and velocity – are subject to classical laws of fluid dynamics whereas at the interfacial surface the fields may be discontinuous and have to satisfy certain "jump conditions", which enforce for instance conservation of mass and momentum. However, in many applications, these interfaces might become very hard to track numerically and their structure very hard to resolve. In particular, when surface tension is included in the model, sharp interface models collapse, in case the topology of the interface becomes singular, which happens when bubbles split or coalesce, cf. [17]. Therefore, phase field models have become an increasingly important tool for the numerical simulation in the last decade. In phase field models, some parameter indicates the distribution of the constituents. This parameter, as well as the fields, varies steeply but smoothly over some interfacial layer, which is thin, but has a nonzero thickness ε. The smoothing effect is achieved by considering energies, which depend on gradients of the fields, an idea going back to [24], which was already applied in [9]. For a review on phase field models in fluid mechanics, we refer to [6]. In the work at hand, we consider a model for a mixture of two incompressible fluids derived in [4]. Both fluids might be transformed into each other by a reaction or a phase transition.

Sharp interface models are physically well–founded and all jump conditions, but the kinetic relation, can be derived from classical conservation considerations. The notion of kinetic relation originates from the theory of solid–solid phase transitions [3], but it can also be applied to more general problems [19]. Phase field models, on the other hand, can be derived using entropy arguments, see [5] for a general framework. Nevertheless, they need to be verified. One important way to do this is to nondimensionalize the system and letting ε go to zero in order to identify physically meaningful sharp interface models.

The work at hand has two interests. The first one is determining the sharp interface limit of two different scalings. We will do this using the technique of formally matched asymptotic expansions, see [8]. Our second aim is to present a numerical scheme to solve an advective Cahn–Hilliard equation which is a subproblem of the whole model. We use a Local Discontinuous Galerkin (LDG) method based on the Dune framework. This type of method is known to handle the discretization of higher order derivatives easily and allows to implement higher order schemes, adaptivity and parallelization in a convenient way. In particular in case of convection dominated problems LDG schemes are superior to continuous Finite Element methods.

1.1. Description of the Model

As pointed out before, the model under consideration is presented in [4], and a detailed derivation is given there. Thus, we will not give many details on the derivation. The model describes a mixture of two incompressible fluids having prescribed density $\tilde{\rho}_1, \tilde{\rho}_2$, respectively. In case these densities coincide the model is fully incompressible and the modeling goes back to [16], see also [14] for a thermodynamically consistent derivation. Different generalizations to the generic case of fluids with different densities, i.e. $\tilde{\rho}_1 \neq \tilde{\rho}_2$, can be found

in [1, 2, 7, 11, 20]. In this case, there is a certain amount of compressibility present in the model. This is due to the fact that the density depends on the mixture ratio of the two fluids.

Let us now give an account of the fields present in the model. By $\varphi \in \mathbb{R}$ we denote the scaled amount of volume occupied by one of the constituents. We have $\varphi = 1$ in case only this constituent is present and $\varphi = -1$ in case it is absent. Hence, the mass densities of the constituents ρ_1, ρ_2 are related to the total mass density $\rho = \rho(\varphi)$ via

$$\rho = \rho_1 + \rho_2 = \tilde{\rho}_1 \frac{1+\varphi}{2} + \tilde{\rho}_2 \frac{1-\varphi}{2}. \tag{1}$$

Furthermore, $\mathbf{v} \in \mathbb{R}^d$ is the mass averaged fluid velocity satisfying

$$\rho \mathbf{v} = \rho_1 \mathbf{v}_1 + \rho_2 \mathbf{v}_2, \tag{2}$$

where $\mathbf{v}_1, \mathbf{v}_2$ are the velocities of the constituents. In addition, the pressure $p = p(\varphi)$ is given via a constitutive relation as a function of φ such that

$$p(\varphi) = \varphi W'(\varphi) - W(\varphi), \tag{3}$$

where $W = W(\varphi)$ is the Helmholtz free energy density. We want to state for later use that (3) implies

$$p'(\varphi) = \varphi W''(\varphi). \tag{4}$$

We impose that the Helmholtz free energy density has a special double–well shape. In particular, we assume

$$W(\varphi) > 0 \quad \forall \varphi \in \mathbb{R} \setminus \{-1, 1\}, \quad \text{and} \quad W(-1) = W(1) = 0 \tag{5}$$

and that there exist $\alpha_1, \alpha_2 \in (-1, 1)$ such that

$$W''(\varphi) > 0 \quad \forall \varphi \in (-\infty, \alpha_1) \cup (\alpha_2, \infty), \quad \text{and} \quad W''(\varphi) < 0 \quad \forall \varphi \in (\alpha_1, \alpha_2). \tag{6}$$

In this way, the Maxwell points of W, which are defined as the values $\varphi^1 < \varphi^2$ satisfying

$$W'(\varphi^1) = W'(\varphi^2) = \frac{W(\varphi^2) - W(\varphi^1)}{\varphi^2 - \varphi^1}, \tag{7}$$

are given by $\varphi^1 = -1$, $\varphi^2 = 1$. We like to point out that because of (4) the nonconvex Helmholtz free energy density implies a nonmonotone pressure function.

The remaining parameters of the model are given as follows: m_J and m_r are the diffusion and reaction mobility, respectively, γ denotes the capillarity coefficient and c_+, c_- are related to the densities $\tilde{\rho}_1$,$\tilde{\rho}_2$ with $\tilde{\rho}_1 < \tilde{\rho}_2$ as follows

$$c_+ = \frac{1}{\tilde{\rho}_1} + \frac{1}{\tilde{\rho}_2}, \qquad c_- = \frac{1}{\tilde{\rho}_1} - \frac{1}{\tilde{\rho}_2}. \tag{8}$$

In addition, let $\Omega \subset \mathbb{R}^d$ be a domain with smooth boundary and $[0, T)$ the time interval of interest. The system, cf. [4], reads in $[0, T) \times \Omega$:

$$\varphi_t + \operatorname{div}(\varphi \mathbf{v}) = c_+(m_J \Delta - m_r)(c_+ \mu + c_- \lambda), \tag{9}$$

$$\rho(\varphi)(\mathbf{v}_t + (\mathbf{v} \cdot \nabla)\mathbf{v}) + \nabla(p(\varphi) + \lambda) = \operatorname{div}(\boldsymbol{\sigma}_{NS}) + \gamma \varphi \nabla \Delta \varphi, \tag{10}$$

$$\operatorname{div}(\mathbf{v}) = c_-(m_J \Delta - m_r)(c_+ \mu + c_- \lambda), \tag{11}$$

where

$$\mu := W'(\varphi) - \gamma \Delta \varphi, \quad p(\varphi) = \varphi W'(\varphi) - W(\varphi), \quad \boldsymbol{\sigma}_{NS} := \eta(\varphi) \operatorname{div}(\mathbf{v}) I + \hat{\eta}(\varphi)(\nabla \mathbf{v} + (\nabla \mathbf{v})^T). \tag{12}$$

The evolution of the model is described by $(\varphi, \mathbf{v}, \lambda)$, where $\lambda \in \mathbb{R}$ presents a Lagrange multiplier, which ensures the incompressibility of the pure constituents. In particular, μ is the chemical potential, $\boldsymbol{\sigma}_{NS}$ is the Navier–Stokes tensor, and η and $\hat{\eta}$ denote the bulk and shear viscosity, respectively, which are interpolated between the two pure constituents.

It is important to note that we have to deal with a rather complicated divergence constraint for the velocity. This is in contrast to the model introduced in [2], where a volume averaged velocity is considered.

To avoid physically meaningless scalings, it is important to nondimensionalize the system before introducing the scaling.

1.2. **Nondimensionalization**

In order to nondimensionalize the system (9)-(12), we introduce the reference quantities $\bar{x}$, $\bar{t}$, $\bar{v}$, $\bar{p}$, $\bar{\lambda}$, $\bar{c}_+$, $\bar{c}_-$, $\bar{\eta}$, $\bar{\gamma}$, $\bar{m}_J$, $\bar{m}_r$, $\bar{\rho}$ such that

$$
\begin{aligned}
&\mathbf{x} = \bar{x}\mathbf{x}^*, && t = \bar{t}t^*, && \mathbf{v} = \bar{v}\mathbf{v}^*, && p = \bar{p}p^*, && \lambda = \bar{\lambda}\lambda^*,\\
&\rho = \bar{\rho}\rho^*, && c_+ = \bar{c}_+c_+^*, && c_- = \bar{c}_-c_-^*, && \eta = \bar{\eta}\eta^*, && \hat{\eta} = \bar{\eta}\hat{\eta}^*,\\
&\gamma = \bar{\gamma}\gamma^*, && m_J = \bar{m}_J m_J^*, && m_r = \bar{m}_r m_r^*, && \mu = \bar{p}\mu^*, && W = \bar{p}W^*.
\end{aligned}
$$

Note that φ is a scaled phase field variable interpolating the density between $\tilde{\rho}_1$ and $\tilde{\rho}_2$, see (1). Hence, it is already dimensionless. Only for reasons of consistent notation, we will use the symbol φ^* instead of φ in the nondimensionalized system. Moreover, we remark that the choices $p = \bar{p}p^*$, $\mu = \bar{p}\mu^*$, and $W = \bar{p}W^*$ are due to the fact that μ and p are quantities that are derived from W, see equation (12). Thus, we recover the nondimensionalized version of the system (9)-(11):

$$
\frac{1}{\bar{t}}\partial_{t^*}\varphi^* + \frac{\bar{v}}{\bar{x}}\operatorname{div}^*(\varphi^*\mathbf{v}^*) - \bar{c}_+c_+^*\left(\frac{\bar{m}_J}{\bar{x}^2}m_J^*\Delta^* - \bar{m}_r m_r^*\right)\left(\bar{c}_+\bar{p}c_+^*\mu^* + \bar{c}_-\bar{\lambda}c_-^*\lambda^*\right) = 0, \tag{13}
$$

$$
\bar{\rho}\rho^*(\varphi^*)\left(\frac{\bar{v}}{\bar{t}}\partial_{t^*}\mathbf{v}^* + \frac{\bar{v}^2}{\bar{x}}(\mathbf{v}^*\cdot\nabla^*)\mathbf{v}^*\right) + \frac{1}{\bar{x}}\nabla^*(\bar{p}p^*(\varphi^*) + \bar{\lambda}\lambda^*) - \frac{\bar{\eta}\bar{v}}{\bar{x}^2}\operatorname{div}^*(\boldsymbol{\sigma}_{NS}^*) - \frac{\bar{\gamma}}{\bar{x}^3}\gamma^*\varphi^*\nabla^*\Delta^*\varphi^* = 0, \tag{14}
$$

$$
\frac{\bar{v}}{\bar{x}}\operatorname{div}^*(\mathbf{v}^*) - \bar{c}_-c_-^*\left(\frac{\bar{m}_J}{\bar{x}^2}m_J^*\Delta^* - \bar{m}_r m_r^*\right)\left(\bar{c}_+\bar{p}c_+^*\mu^* + \bar{c}_-\bar{\lambda}c_-^*\lambda^*\right) = 0. \tag{15}
$$

For the consitutive laws, we clearly have $p = \bar{p}p^*$ and obtain

$$
\boldsymbol{\sigma}_{NS}^* := \eta^*(\varphi^*)\operatorname{div}^*(\mathbf{v}^*)I + \hat{\eta}^*(\varphi^*)(\nabla^*\mathbf{v}^* + (\nabla^*\mathbf{v}^*)^T), \qquad \bar{p}\mu^* = \bar{p}(W^*)'(\varphi^*) + \frac{\bar{\gamma}}{\bar{x}^2}\gamma^*\Delta^*\varphi^*. \tag{16}
$$

We denote by M the Mach number and by Re the Reynolds number, which are given by $\mathrm{M} = \bar{v}\sqrt{\frac{\bar{\rho}}{\bar{p}}}$, and $\mathrm{Re} = \frac{\bar{\rho}\bar{v}\bar{x}}{\bar{\eta}}$, respectively. By the definitions of c_+ and c_-, see (8), it is reasonable to choose $\bar{c}_+ = \frac{1}{\bar{\rho}}$ and $\bar{c}_- = \frac{\bar{q}}{\bar{\rho}}$, where $\bar{q}$ is an additional reference quantity, that measures the difference between the densities $\tilde{\rho}_1$ and $\tilde{\rho}_2$ in the following sense

$$
\bar{q} = \frac{\tilde{\rho}_2 - \tilde{\rho}_1}{\tilde{\rho}_1\tilde{\rho}_2}\bar{\rho} = \frac{\hat{\rho}_2 - \hat{\rho}_1}{\hat{\rho}_1\hat{\rho}_2}, \quad \text{where} \quad \hat{\rho}_i = \frac{\tilde{\rho}_i}{\bar{\rho}} \quad \text{for} \quad i = 1, 2. \tag{17}
$$

For the reference velocity $\bar{v}$, we make the choice $\bar{v} = \frac{\bar{x}}{\bar{t}}$, although other physically reasonable scalings, like e.g. $\bar{v} = \sqrt{\frac{\bar{p}}{\bar{\rho}}}$, exist. Our choice ensures that $\partial_{t^*}\varphi^*$ and $\mathrm{div}^*(\varphi^* v^*)$ appear in the same order. Therefore, we get

$$\partial_{t^*}\varphi^* + \mathrm{div}^*(\varphi^*\mathbf{v}^*) - \frac{\bar{t}\bar{p}}{\bar{\rho}^2}c_+^*\left(\frac{\bar{m}_J}{\bar{x}^2}m_J^*\Delta^* - \bar{m}_r m_r^*\right)\left(c_+^*\mu^* + \bar{q}c_-^*\frac{\bar{\lambda}}{\bar{p}}\lambda^*\right) = 0, \quad (18)$$

$$\rho^*(\varphi^*)\left(\partial_{t^*}\mathbf{v}^* + (\mathbf{v}^*\cdot\nabla^*)\mathbf{v}^*\right) + \frac{1}{\mathrm{M}^2}\nabla^*\left(p^*(\varphi^*) + \frac{\bar{\lambda}}{\bar{p}}\lambda^*\right) - \frac{1}{\mathrm{Re}}\mathrm{div}^*(\boldsymbol{\sigma}_{NS}^*) - \frac{\bar{\gamma}}{\mathrm{M}^2\bar{x}^2\bar{p}}\gamma^*\varphi^*\nabla^*\Delta^*\varphi^* = 0, \quad (19)$$

$$\mathrm{div}^*(\mathbf{v}^*) - \frac{\bar{t}\bar{p}\bar{q}}{\bar{\rho}^2}c_-^*\left(\frac{\bar{m}_J}{\bar{x}^2}m_J^*\Delta^* - \bar{m}_r m_r^*\right)\left(c_+^*\mu^* + \bar{q}c_-^*\frac{\bar{\lambda}}{\bar{p}}\lambda^*\right) = 0, \quad (20)$$

and

$$\mu^* = (W^*)'(\varphi^*) + \frac{\bar{\gamma}}{\bar{x}^2\bar{p}}\gamma^*\Delta^*\varphi^*. \quad (21)$$

We introduce a small parameter $\varepsilon > 0$, representing the width of the interface, such that

$$\varepsilon = \sqrt{\frac{\bar{\gamma}}{\bar{x}^2\bar{p}}}. \quad (22)$$

This is justified by the following remark.

Remark 1.1 (Interfacial thickness)**.** The fact that ε, see (22), represents the thickness of the interface may be justified by constructing recovery sequences for the Γ–limit of the energy functional

$$\int_\Omega \frac{1}{\sqrt{\bar{\gamma}}}W(\varphi) + \sqrt{\bar{\gamma}}\,|\nabla\varphi|^2\,\mathrm{d}\mathbf{x} \quad \text{as } \sqrt{\bar{\gamma}} \to 0,$$

see [21, 23].

In addition to (22), we choose the following scalings

$$\bar{q} = 1, \quad \frac{\bar{t}\bar{p}\bar{m}_J}{\bar{\rho}^2\bar{x}^2} = \frac{1}{\varepsilon}, \quad \bar{m}_r = 0, \quad \text{and} \quad \frac{\bar{\lambda}}{\bar{p}} = 1. \quad (23)$$

Finally, inserting the scalings (22) and (23) into the system (18)-(21) leads to

$$\partial_{t^*}\varphi^* + \mathrm{div}^*(\varphi^*\mathbf{v}^*) = \frac{1}{\varepsilon}c_+^* m_J^*\Delta^*\left(c_+^*\mu^* + c_-^*\lambda^*\right), \quad (24)$$

$$\rho^*(\varphi^*)\left(\partial_{t^*}\mathbf{v}^* + (\mathbf{v}^*\cdot\nabla^*)\mathbf{v}^*\right) + \frac{1}{\mathrm{M}^2}\nabla^*\left(p^*(\varphi^*) + \lambda^*\right) = \frac{1}{\mathrm{Re}}\mathrm{div}^*(\boldsymbol{\sigma}_{NS}^*) + \frac{\varepsilon^2}{\mathrm{M}^2}\gamma^*\varphi^*\nabla^*\Delta^*\varphi^*, \quad (25)$$

$$\mathrm{div}^*(\mathbf{v}^*) = \frac{1}{\varepsilon}c_-^* m_J^*\Delta^*\left(c_+^*\mu^* + c_-^*\lambda^*\right). \quad (26)$$

We only give the consitutive equation for μ as it is the only one containing ε:

$$\mu^* = (W^*)'(\varphi^*) - \varepsilon^2\gamma^*\Delta^*\varphi^*. \quad (27)$$

In this paper, for the remaining quantities, we will study the following two scalings

$$\mathrm{Re} = 1, \quad \text{and} \quad \mathrm{M} = \varepsilon, \quad (28)$$

$$\mathrm{Re} = \frac{1}{\varepsilon}, \quad \text{and} \quad \mathrm{M} = \sqrt{\varepsilon}, \quad (29)$$

which we call **strong capillarity regime**, and **low viscosity regime**, respectively. For these scalings, we will study the comportment of solutions of the system (24)-(27), when the parameter ε tends to 0. This will be carried out by the technique of matched asymptotic expansions in section 5. For convenience, we will omit the symbol * in the sequel. Note that in the context of Navier–Stokes–Korteweg systems, the zero Mach number limit has been considered in [15].

1.3. **Results**

The paper is organized as follows. We first show that the model dissipates energy, see section 2. Section 3 describes a general framework of sharp interface models. Then, we recall several results and definitions from the theory of matched asymptotic expansions in section 4. In the main part, section 5, we determine the sharp interface limits of the two different scalings in (28) and (29). In subsection 5.1, we present a scaling where the capillarity effects are so strong that the mean curvature of the phase boundary has to be constant, while in the second scaling, see subsection 5.2, the Navier–Stokes tensor vanishes in the limit. Finally, we present a numerical treatment of a part of the model in section 6. We have implemented a Local Discontinuous Galerkin scheme for the Cahn–Hilliard equation with a convection term, which governs the evolution of the phase field variable. We show that the scheme has the expected order of approximation in the one–dimesional case. We give two examples in two dimensions to demonstrate the expected behavior in the case with and without an additional advection term.

2. Entropy Inequality

In this section, we will prove that the isothermal model at hand dissipates energy, which is equivalent to the fact that it is compatible with the second law of thermodynamics. Basically, this follows from the construction of the model via a suitable decomposition of the entropy dissipation into a sum of fluxes and driving forces, see [4] for details. However, we think that, for completeness of this article, the entropy inequality should be stated and proven. In particular, it will become clear in which way the energy contains gradients of the phase field function. These terms act as a penalty for steep gradients and enforce the smooth transition from one phase to the other. In addition, the entropy inequality can be seen as a first (small) step to establish stability of the model. As the energy dissipation of the model does not depend on the scaling, we consider (9)-(12) instead of any scaled version. In particular, our discussion includes the case $m_r \neq 0$.

We start by providing some properties of smooth solutions of the system (9)-(12) for later use.

Remark 2.1. Let $(\varphi, \mathbf{v}, \lambda)$ be a smooth solution of the system (9)-(12).

(1) By combining (9) and (11), we find

$$\varphi_t + \operatorname{div}(\varphi \mathbf{v}) = c_+ m_J \Delta(c_+\mu + c_-\lambda) - c_+ m_r (c_+\mu + c_-\lambda) = \frac{c_+}{c_-} \operatorname{div}(\mathbf{v}). \tag{30}$$

(2) From (1), (8), and (30) follows, that mass conservation is valid, i.e.

$$\rho(\varphi)_t + \operatorname{div}(\rho(\varphi)\mathbf{v}) = 0. \tag{31}$$

To see that the system (9)-(12) is physically meaningful, we have to check that its solutions satisfy the balance of momentum for an appropriate stress tensor.

Remark 2.2. In [13], a thermodynamically consistent Korteweg stress tensor $\boldsymbol{\sigma}_K$ with temperature is introduced which reduces for isothermal processes to $\boldsymbol{\sigma}_K = \gamma(\varphi\Delta\varphi + \frac{1}{2}|\nabla\varphi|^2)I - \gamma\nabla\varphi \otimes \nabla\varphi$. Since $\operatorname{div}(\boldsymbol{\sigma}_K) = \gamma\varphi\nabla\Delta\varphi$, for this choice the balance of momentum reads

$$(\rho(\varphi)\mathbf{v})_t + \operatorname{div}(\rho(\varphi)\mathbf{v}\otimes\mathbf{v}) + \nabla(p(\varphi)+\lambda) = \operatorname{div}(\boldsymbol{\sigma}_{NS}) + \operatorname{div}(\boldsymbol{\sigma}_K) = \operatorname{div}(\boldsymbol{\sigma}_{NS}) + \gamma\varphi\nabla\Delta\varphi, \tag{32}$$

which, in view of (31), is equation (10).

Theorem 2.3. *Let $\Omega \subset \mathbb{R}^d$ be a domain with smooth boundary and $(\varphi, \mathbf{v}, \lambda)$ be a smooth solution of the system (9)-(12) satisfying the boundary conditions*

$$\nabla\varphi \cdot \boldsymbol{\nu} = 0, \quad \mathbf{v} \cdot \boldsymbol{\nu} = 0, \quad \textit{and} \quad \nabla(c_+\mu + c_-\lambda) \cdot \boldsymbol{\nu} = 0 \tag{33}$$

on $[0,T) \times \partial\Omega$. Then, the total energy is nonincreasing, i.e.

$$\begin{aligned}\frac{\mathrm{d}}{\mathrm{d}t}\left(\int_\Omega W(\varphi) + \tfrac{1}{2}\gamma\left|\nabla\varphi\right|^2 + \tfrac{1}{2}\rho(\varphi)\left|\mathbf{v}\right|^2 \mathrm{d}\mathbf{x}\right)\\ = -\int_\Omega m_J|\nabla(c_+\mu + c_-\lambda)|^2 + m_r(c_+\mu + c_-\lambda)^2 + \boldsymbol{\sigma}_{NS} : \nabla\mathbf{v}\,\mathrm{d}\mathbf{x} \le 0.\end{aligned} \tag{34}$$

Proof. The energy density $e = e(\varphi, \nabla\varphi, \mathbf{v}) := W(\varphi) + \frac{1}{2}\gamma\left|\nabla\varphi\right|^2 + \frac{1}{2}\rho(\varphi)\left|\mathbf{v}\right|^2$ possesses the time derivative $e_t = W'(\varphi)\varphi_t + \gamma\nabla\varphi\cdot\nabla\varphi_t + \mathbf{v}\cdot(\rho(\varphi)\mathbf{v})_t - \frac{1}{2}\left|\mathbf{v}\right|^2\rho(\varphi)_t$. If we replace all time derivatives with the help of (30), (31), and (32), we get

$$\begin{aligned}e_t =& W'(\varphi)\left(\tfrac{c_+}{c_-}\operatorname{div}(\mathbf{v}) - \operatorname{div}(\varphi\mathbf{v})\right) + \gamma\nabla\varphi\cdot\nabla\left(\tfrac{c_+}{c_-}\operatorname{div}(\mathbf{v}) - \operatorname{div}(\varphi\mathbf{v})\right) + \mathbf{v}\cdot(\operatorname{div}(\boldsymbol{\sigma}_{NS}) + \operatorname{div}(\boldsymbol{\sigma}_K))\\ &- \mathbf{v}\cdot\nabla\left(p(\varphi) + \lambda\right) - \frac{1}{2}\operatorname{div}\left(\rho\left|\mathbf{v}\right|^2\mathbf{v}\right).\end{aligned}$$

Abbreviating $A := e_t + \operatorname{div}(e\mathbf{v}) + \operatorname{div}((p(\varphi)I - \boldsymbol{\sigma}_{NS} - \boldsymbol{\sigma}_K)\mathbf{v})$ yields

$$\begin{aligned}A =& W'(\varphi)\left(\tfrac{c_+}{c_-}\operatorname{div}(\mathbf{v}) - \operatorname{div}(\varphi\mathbf{v})\right) + \gamma\nabla\varphi\cdot\nabla\left(\tfrac{c_+}{c_-}\operatorname{div}(\mathbf{v}) - \operatorname{div}(\varphi\mathbf{v})\right) - \boldsymbol{\sigma}_{NS} : \nabla\mathbf{v} - \boldsymbol{\sigma}_K : \nabla\mathbf{v}\\ &- \mathbf{v}\cdot\nabla\lambda + (p(\varphi) + W(\varphi))\operatorname{div}(\mathbf{v}) + \nabla W(\varphi)\cdot\mathbf{v} + \frac{1}{2}\gamma\operatorname{div}(\left|\nabla\varphi\right|^2\mathbf{v}).\end{aligned}$$

After some rearrangements, using (3), this reduces to

$$A = \tfrac{c_+}{c_-}W'(\varphi)\operatorname{div}(\mathbf{v}) + \tfrac{c_+}{c_-}\gamma\nabla\varphi\cdot\nabla\operatorname{div}(\mathbf{v}) - \boldsymbol{\sigma}_{NS} : \nabla\mathbf{v} - \mathbf{v}\cdot\nabla\lambda - \gamma\operatorname{div}(\operatorname{div}(\mathbf{v})\varphi\nabla\varphi).$$

Now, we integrate over A. Making use of the boundary conditions (33) and recalling (12) and (30), we obtain

$$\begin{aligned}\frac{\mathrm{d}}{\mathrm{d}t}\left(\int_\Omega e\,\mathrm{d}\mathbf{x}\right) &= \int_\Omega \left[\tfrac{c_+}{c_-}(W'(\varphi) - \gamma\Delta\varphi) + \lambda\right]\operatorname{div}(\mathbf{v}) - \boldsymbol{\sigma}_{NS} : \nabla\mathbf{v}\,\mathrm{d}\mathbf{x}\\ &= -\int_\Omega m_J|\nabla(c_+\mu + c_-\lambda)|^2 + m_r(c_+\mu + c_-\lambda)^2 + \boldsymbol{\sigma}_{NS} : \nabla\mathbf{v}\,\mathrm{d}\mathbf{x}.\end{aligned}$$

□

3. Sharp Interface Setting

This section is devoted to describe a general framework for sharp interface models, into which the sharp interface limits derived in section 5 have to fit.

For notational simplicity, we consider the two–dimensional case. We are convinced that our sharp interface limits already discover all information on the bulk equations and jump conditions in this case and the notational burden of considerations in higher dimensions would not be justified.

We consider a C^2–hypersurface $\Gamma(t)$, $t \in [0,T)$. Any point of $\Gamma(t)$ is given by the function $\mathbf{r}(t,s)$, where $s \in I \subset \mathbb{R}$, I bounded interval, is used to parameterize $\Gamma(t)$, i. e. $\mathbf{r} : [0,T) \times I \to \mathbb{R}^2$. A two–phase body $\Omega \subset \mathbb{R}^2$

is decomposed by the *interface* $\Gamma(t)$ into two bulk phases $\Omega^+(t)$ and $\Omega^-(t)$, i.e. we have $\Omega = \Omega^+(t) \cup \Omega^-(t) \cup \Gamma(t)$, $t \in [0,T)$.

We assign to Ω a generic additive quantity $\Psi(t)$, which is represented by

$$\Psi(t) = \int_{\Omega^+(t)} \psi(t,\mathbf{x})\,\mathrm{d}\mathbf{x} + \int_{\Omega^-(t)} \psi(t,\mathbf{x})\,\mathrm{d}\mathbf{x} + \int_I \psi_\Gamma(t,s)\,\mathrm{d}s,$$

where ψ and ψ_Γ are the corresponding densities of Ψ. The quantity ψ may change due to fluxes and sources. This is locally described by equations of balance for the densities. In $\Omega^\pm(t)$, the equations of balance read

$$\frac{\partial \psi}{\partial t} + \operatorname{div}(\psi \mathbf{v} + \mathbf{f}) = \xi,$$

where $\mathbf{v} : [0,T) \times \Omega^\pm \to \mathbb{R}^2$ is the fluid velocity, $\mathbf{f} : [0,T) \times \Omega^\pm \to \mathbb{R}^2$ denotes a nonconvective flux and $\xi : [0,T) \times \Omega^\pm \to \mathbb{R}$ is a source density. On the interface $\Gamma(t)$, we have

$$-w_\nu [\![\psi]\!] + [\![\psi \mathbf{v} + \mathbf{f}]\!] \cdot \boldsymbol{\nu} = -\frac{\partial \psi_\Gamma}{\partial t} - \psi_\Gamma(\operatorname{div}_\Gamma(w_t \mathbf{t}) - \kappa w_\nu) - \operatorname{div}_\Gamma(\mathbf{f}_\Gamma) + \xi_\Gamma. \tag{35}$$

The newly introduced quantities are the interface normal $\boldsymbol{\nu} : [0,T) \times I \to \mathbb{R}^2$, the interface velocity $\mathbf{w} : [0,T) \times I \to \mathbb{R}^2$, which is decomposed into normal and tangential components, i. e. w_ν and w_t (see (39)), the interface flux $\mathbf{f}_\Gamma : [0,T) \times I \to \mathbb{R}^2$ and the interface source $\xi_\Gamma : [0,T) \times I \to \mathbb{R}$. Double brackets $[\![\cdot]\!]$ denote the difference of a bulk quantity at the left and right side of the interface and $\operatorname{div}_\Gamma$ is the surface divergence.

In section 5, we will derive interface conditions from the diffuse interface model. For proper choices of the generic quantities that are introduced here, these conditions have to fit into the given sharp interface setting (35).

4. Asymptotic Analysis

4.1. **Decomposition of the Domain**

We decompose the given physical domain $\Omega \subset \mathbb{R}^2$ into two bulk regions $\Omega^+(t;\varepsilon)$ and $\Omega^-(t;\varepsilon)$, which are separated by an interfacial surface $\Gamma(t;\varepsilon)$, $\varepsilon > 0$ small. The interface $\Gamma(t;\varepsilon)$ is assumed to be a smoothly evolving $\mathrm{C}^1([0,T), \mathrm{C}^2(\Omega))$–hypersurface which is defined by

$$\Gamma(t,\varepsilon) := \{x \in \Omega : \varphi_\varepsilon(t,\mathbf{x}) = 0\},$$

where φ_ε is the solution of (24)-(27). The bulk domains are given by

$$\Omega^-(t,\varepsilon) := \{\mathbf{x} \in \Omega \ : \ \varphi_\varepsilon(t,\mathbf{x}) < 0\} \quad \text{and} \quad \Omega^+(t,\varepsilon) := \{\mathbf{x} \in \Omega \ : \ \varphi_\varepsilon(t,\mathbf{x}) > 0\}.$$

We assume that a limiting curve $\Gamma = \Gamma(t)$ exists when ε tends to zero. The corresponding bulk domains are abbreviated by $\Omega^-(t)$ and $\Omega^+(t)$.

In the sequel, we will consider the so called outer setting in the bulk domains and the so called inner setting in a neighborhood of $\Gamma(t)$.

4.2. **Outer Setting**

Another main assumption of formally matched asymptotics is that all quantities have asymptotic expansions in the small parameter ε, which is related to the thickness of the interfacial layer, cf. Remark 1.1 for details.

We assume the existence of the following expansions for the velocity $\mathbf{v}$, the phase field parameter φ and the Lagrange multiplier λ in the bulk domains $\Omega^{\pm}(t,\varepsilon)$:

$$\mathbf{v}(t,\mathbf{x};\varepsilon) = \mathbf{v}_0(t,\mathbf{x}) + \varepsilon \mathbf{v}_1(t,\mathbf{x}) + o(\varepsilon), \tag{36}$$

$$\varphi(t,\mathbf{x};\varepsilon) = \varphi_0(t,\mathbf{x}) + \varepsilon \varphi_1(t,\mathbf{x}) + \varepsilon^2 \varphi_2(t,\mathbf{x}) + o(\varepsilon^2), \tag{37}$$

$$\lambda(t,\mathbf{x};\varepsilon) = \lambda_0(t,\mathbf{x}) + \varepsilon \lambda_1(t,\mathbf{x}) + \varepsilon^2 \lambda_2(t,\mathbf{x}) + o(\varepsilon^2). \tag{38}$$

These expansions will be inserted in the scaled equations to obtain the equations satisfied by outer solutions, cf. e.g. Definition 5.1.

4.3. **Inner Setting**

The position of the limiting phase boundary $\Gamma(t)$ is given as a function $\mathbf{r}(t,s)$, where $I \subset \mathbb{R}$ is some bounded interval which we use as parameter domain and $s \in I$ is used to parameterize the interface. From the map $\mathbf{r}$, we can compute tangent and normal vectors to the interface as well as the interface velocity. The tangent vector pointing in counterclockwise direction and the unit normal to the interface pointing to the left of the curve are given by

$$\mathbf{t}(t,s) = \left(\frac{\partial r^1}{\partial s}(t,s), \frac{\partial r^2}{\partial s}(t,s)\right)^T, \quad \text{and} \quad \boldsymbol{\nu}(t,s) = \frac{1}{|\mathbf{t}(t,s)|}\left(-\frac{\partial r^2}{\partial s}(t,s), \frac{\partial r^1}{\partial s}(t,s)\right)^T,$$

respectively, where r^1, r^2 denote the components of $\mathbf{r}$ in Cartesian coordinates. In the following, we abbreviate the partial derivative of a quantity l with respect to s by l_s. The mean curvature κ is defined by

$$\kappa = \frac{r_s^1 r_{ss}^2 - r_{ss}^1 r_s^2}{((r_s^1)^2 + (r_s^2)^2)^{\frac{3}{2}}}.$$

The interface velocity, which is defined as the time derivative of $\mathbf{r}$, can be decomposed into tangential and normal components by

$$\mathbf{w} = \frac{\partial \mathbf{r}}{\partial t} = w_t \mathbf{t} + w_\nu \boldsymbol{\nu}. \tag{39}$$

There are some identities linking s–derivatives of $\mathbf{t}$ and $\boldsymbol{\nu}$ with κ :

$$\left(\frac{t^j}{|\mathbf{t}|}\right)_s = \kappa |\mathbf{t}| \nu^j \quad \text{and} \quad (\nu^j)_s = -t^j \kappa \quad \text{for } j = 1,2.$$

To each $t \in [0,T)$, there exists some neighborhood $\mathcal{N}(t) \subset \Omega$ of $\Gamma(t)$ such that every point $(x^1,x^2) \in \mathcal{N}(t)$ can be represented as

$$\begin{pmatrix} x^1 \\ x^2 \end{pmatrix}(\tau,s,z) = \mathbf{r}(\tau,s) + \varepsilon z \boldsymbol{\nu}(\tau,s), \quad \tau = t. \tag{40}$$

Thus, z is the scaled distance from the interface in normal direction. The small parameter ε is introduced here to zoom into the interfacial region. We use (40) to change variables from (t,x^1,x^2) to (τ,s,z). For a scalar or a Cartesian component of a vector ψ, which is defined in inner and outer coordinates, i.e. $\psi(t,x^1,x^2) = \Psi(\tau,s,z)$, the partial derivatives transform as follows:

$$\begin{pmatrix} \frac{\partial \psi}{\partial x^1} \\ \frac{\partial \psi}{\partial x^2} \\ \frac{\partial \psi}{\partial t} \end{pmatrix} = \begin{pmatrix} (1+\varepsilon z\kappa)\frac{1}{|\mathbf{t}|^2} t^1 & \varepsilon^{-1}\nu^1 & 0 \\ (1+\varepsilon z\kappa)\frac{1}{|\mathbf{t}|^2} t^2 & \varepsilon^{-1}\nu^2 & 0 \\ -(1+\varepsilon z\kappa)(w_t + \varepsilon z \frac{1}{|\mathbf{t}|^2} t^i (\nu^i)_\tau) & -\varepsilon^{-1} w_\nu & 1 \end{pmatrix} \begin{pmatrix} \frac{\partial \Psi}{\partial s} \\ \frac{\partial \Psi}{\partial z} \\ \frac{\partial \Psi}{\partial \tau} \end{pmatrix} + \mathcal{O}(\varepsilon^2), \tag{41}$$

for a fixed point (τ, s, z). The derivation of (41) can be found in e.g. [12]. In accordance with (36)-(38), we assume that the quantities in inner variables can also be expanded in ε :

$$\mathbf{V}(\tau, s, z; \varepsilon) = \mathbf{V}_0(\tau, s, z) + \varepsilon \mathbf{V}_1(\tau, s, z) + o(\varepsilon), \tag{42}$$

$$\Phi(\tau, s, z; \varepsilon) = \Phi_0(\tau, s, z) + \varepsilon \Phi_1(\tau, s, z) + \varepsilon^2 \Phi_2(\tau, s, z) + o(\varepsilon^2), \tag{43}$$

$$\Lambda(\tau, s, z; \varepsilon) = \Lambda_0(\tau, s, z) + \varepsilon \Lambda_1(\tau, s, z) + \varepsilon^2 \Lambda_2(\tau, s, z) + o(\varepsilon^2). \tag{44}$$

By using (41) and plugging (42)-(44) into the scaled systems, we obtain the equations satisfied by the inner solutions, cf. e.g. (65)-(70) and Definition 5.2, by comparing coefficients of different powers of ε.

4.4. **Matching Conditions**

Inner and outer quantities are matched by the usual procedure, see [8,12] for details. However, for convenience of the reader, we recall the matching conditions, one obtains up to second order. Note that we use Einstein summation convention:

$$\Psi_0(\tau, s, z) \to \psi_0^{\pm}(\tau, \mathbf{r}(\tau, s)) \quad z \to \pm\infty, \tag{45}$$

$$\Psi_1(\tau, s, z) - \left(\frac{\partial \psi_0}{\partial x^j}\right)^{\pm} (\tau, \mathbf{r}(\tau, s)) \nu^j(\tau, s) z \to \psi_1^{\pm}(\tau, \mathbf{r}(\tau, s)) \quad z \to \pm\infty, \tag{46}$$

$$\Psi_2(\tau, s, z) - \frac{1}{2} z^2 \left(\frac{\partial^2 \psi_0}{\partial x^i \partial x^j}\right)^{\pm} (\tau, \mathbf{r}(\tau, s)) \nu^i \nu^j - \frac{1}{2} z \left(\frac{\partial \psi_1}{\partial x^i}\right)^{\pm} (\tau, \mathbf{r}(\tau, s)) \nu^i \to \psi_2^{\pm}(\tau, \mathbf{r}(\tau, s)) \quad z \to \pm\infty. \tag{47}$$

We also get conditions for the derivatives which are basically derived by differentiating the equations leading to the above conditions.

$$\Psi_{0,\tau} \to \left(\frac{\partial \psi_0}{\partial x^j}\right)^{\pm} (\tau, \mathbf{r}(\tau, s)) w^j(\tau, s) + \left(\frac{\partial \psi_0}{\partial t}\right)^{\pm} (\tau, \mathbf{r}(\tau, s)) \quad z \to \pm\infty, \tag{48}$$

$$\Psi_{0,s} \to \left(\frac{\partial \psi_0}{\partial x^j}\right)^{\pm} (\tau, \mathbf{r}(\tau, s)) t^j(\tau, s) \quad z \to \pm\infty, \tag{49}$$

$$\Psi_{1,z} \to \left(\frac{\partial \psi_0}{\partial x^j}\right)^{\pm} (\tau, \mathbf{r}(\tau, s)) \nu^j(\tau, s) \quad z \to \pm\infty, \tag{50}$$

$$\Psi_{0,z}, \Psi_{0,zz}, \Psi_{1,zz} \to 0 \quad z \to \pm\infty, \tag{51}$$

$$\Psi_{2,z} - z \left(\frac{\partial^2 \psi_0}{\partial x^i \partial x^j}\right)^{\pm} (\tau, \mathbf{r}(\tau, s)) \nu^i \nu^j \to \frac{1}{2} \left(\frac{\partial \psi_1}{\partial x^i}\right)^{\pm} (\tau, \mathbf{r}(\tau, s)) \nu^i(\tau, s) \quad z \to \pm\infty, \tag{52}$$

$$\Psi_{2,zz} \to \left(\frac{\partial^2 \psi_0}{\partial x^i \partial x^j}\right)^{\pm} (\tau, \mathbf{r}(\tau, s)) \nu^i(\tau, s) \nu^j(\tau, s) \quad z \to \pm\infty. \tag{53}$$

We impose that all these limits are attained superlinearly fast.

5. Derivation of the Sharp Interface Limits

In (28) and (29), we have suggested two scalings of the system (24)-(27). In this section, we will explore the sharp interface limits for these scalings.

5.1. **Strong Capillarity Scaling**

In this section, we will consider a scaling with extremely strong capillary effects. We will see that the sharp interface limit problem is given by the incompressible Navier–Stokes equations, subject to a Young–Laplace

condition for the jump of a lower order pressure than the one present in the momentum balance. The extremely strong capillary effects enforce interfaces of constant mean curvature. The scaled system corresponds to very small Mach numbers, i.e. $\mathrm{M} \sim \varepsilon$, and high mobilities and reads

$$\varphi_t + \operatorname{div}(\varphi \mathbf{v}) = \frac{1}{\varepsilon} c_+ m_J \Delta(c_+\mu + c_-\lambda), \tag{54}$$

$$\rho(\varphi)(\mathbf{v}_t + (\mathbf{v}\cdot\nabla)\mathbf{v}) + \frac{1}{\varepsilon^2}\nabla(p(\varphi)+\lambda) = \operatorname{div}(\boldsymbol{\sigma}_{NS}) + \gamma\varphi\nabla\Delta\varphi, \tag{55}$$

$$\operatorname{div}(\mathbf{v}) = \frac{1}{\varepsilon} c_- m_J \Delta(c_+\mu + c_-\lambda), \tag{56}$$

with the constitutive laws

$$\mu = W'(\varphi) - \gamma\varepsilon^2\Delta\varphi, \quad p(\varphi) = \varphi W'(\varphi) - W(\varphi), \quad \boldsymbol{\sigma}_{NS} = \eta(\varphi)\operatorname{div}(\mathbf{v})I + \hat{\eta}(\varphi)(\nabla\mathbf{v} + (\nabla\mathbf{v})^T). \tag{57}$$

The equations for $(\lambda_0, \mathbf{v}_0, \varphi_0, \lambda_1, \varphi_1)$ in the bulk phases are obtainded, by plugging expansions (36)-(38) into (54)-(56) and by gathering terms having the same order in ε. Hence, we have in order ε^{-2}

$$0 = \nabla(p(\varphi_0) + \lambda_0), \tag{58}$$

in order ε^{-1}

$$0 = \Delta(c_+\mu_0 + c_-\lambda_0), \tag{59}$$

$$0 = \nabla(p'(\varphi_0)\varphi_1 + \lambda_1), \tag{60}$$

and in order ε^0

$$\varphi_{0,t} + \operatorname{div}(\varphi_0\mathbf{v}_0) = c_+ m_J \Delta(c_+\mu_1 + c_-\lambda_1), \tag{61}$$

$$\operatorname{div}(\mathbf{v}_0) = c_- m_J \Delta(c_+\mu_1 + c_-\lambda_1). \tag{62}$$

In addition, we find by using the expansions in (57)

$$\mu_0 := W'(\varphi_0), \quad \mu_1 := W''(\varphi_0)\varphi_1, \quad p_0 = p(\varphi_0), \quad p_1 = p'(\varphi_0)\varphi_1. \tag{63}$$

We want to stress that (57) are definitions, in contrast to equations (54)-(56). Thus, we cannot prescribe an expansion for μ, but the expansion of μ is prescribed by (57) and the expansion of φ. These equations motivate the following definition.

Definition 5.1 (Outer solution)**.** A tuple $(\lambda_0, \mathbf{v}_0, \varphi_0, \lambda_1, \varphi_1)$ such that

$$\begin{aligned}
&\lambda_0, \varphi_1, \lambda_1 \in \mathrm{C}^0([0,T), \mathrm{C}^2(\bar{\Omega}^{\pm}(t), \mathbb{R})),\\
&\quad \varphi_0 \in \mathrm{C}^1([0,T), \mathrm{C}^0(\bar{\Omega}^{\pm}(t), \mathbb{R})) \cap \mathrm{C}^0([0,T), \mathrm{C}^2(\bar{\Omega}^{\pm}(t), \mathbb{R})),\\
&\quad \mathbf{v}_0 \in \mathrm{C}^0([0,T), \mathrm{C}^1(\bar{\Omega}^{\pm}(t), \mathbb{R}^2)),
\end{aligned}$$

is called an **outer solution of the strong capillarity regime** provided it satisfies (58)-(62), where μ_0, μ_1 are given by (63), and $\varphi_0 \not\equiv \frac{c_+}{c_-}$. In addition, the boundary condition

$$\nabla\varphi_0 \cdot \boldsymbol{\nu} = 0 \text{ on } [0,T) \times \partial\Omega \tag{64}$$

has to be satisfied.

The inner equations are obtained as follows: We perform the coordinate transformation given by (40) in (54)-(56). Then, we plug in the expansions in inner coordinates (42)-(44). Finally, we gather terms of the same order of ε, which yields

$$
\begin{aligned}
(c_+M_0 + c_-\Lambda_0)_{zz} =& 0, && (65)\\
(p(\Phi_0) + \Lambda_0)_z =& \gamma\Phi_0\Phi_{0,zzz}, && (66)\\
(c_+M_1 + c_-\Lambda_1)_{zz} - \kappa(c_+M_0 + c_-\Lambda_0)_z =& 0, && (67)\\
(p(\Phi_0)\Phi_1 + \Lambda_1)_z\boldsymbol{\nu} + (p(\Phi_0) + \Lambda_0)_s\frac{\mathbf{t}}{\|\mathbf{t}\|^2} =& ((\eta(\Phi_0) + 2\hat{\eta}(\Phi_0))\mathbf{V}_{0,z}\cdot\boldsymbol{\nu})_z\boldsymbol{\nu} + (\hat{\eta}(\Phi_0)\mathbf{V}_{0,z}\cdot\frac{\mathbf{t}}{\|\mathbf{t}\|^2})_z\mathbf{t} && (68)\\
&+ \gamma(\Phi_1\Phi_{0,zzz} + \Phi_0\Phi_{1,zzz} - \kappa\Phi_0\Phi_{0,zz})\boldsymbol{\nu} + \gamma\Phi_0\Phi_{0,zzs}\frac{\mathbf{t}}{\|\mathbf{t}\|^2},\\
-w_\nu\Phi_{0,z} + (\Phi_0\mathbf{V}_0\cdot\boldsymbol{\nu})_z =& c_+m_J\big[(c_+M_2 + c_-\Lambda_2)_{zz} - \kappa(c_+M_1 + c_-\Lambda_1)_z && (69)\\
&+ (c_+M_0 + c_-\Lambda_0)_{ss} - z\kappa^2(c_+M_0 + c_-\Lambda_0)_z\big],\\
\frac{c_+}{c_-}(\mathbf{V}_0\cdot\boldsymbol{\nu})_z =& c_+m_J\big[(c_+M_2 + c_-\Lambda_2)_{zz} - \kappa(c_+M_1 + c_-\Lambda_1)_z && (70)\\
&+ (c_+M_0 + c_-\Lambda_0)_{ss} - z\kappa^2(c_+M_0 + c_-\Lambda_0)_z\big].
\end{aligned}
$$

Furthermore, doing the same for (57) gives

$$
\begin{aligned}
&P_0 = p(\Phi_0), \qquad P_1 = p'(\Phi_0)\Phi_1,\\
&M_0 = W'(\Phi_0) - \gamma\Phi_{0,zz}, \qquad M_1 = W''(\Phi_0)\Phi_1 - \gamma\Phi_{1,zz} + \gamma\kappa\Phi_{0,z},\\
&M_2 = W''(\Phi_0)\Phi_2 + \frac{1}{2}W'''(\Phi_0)\Phi_1^2 - \gamma\Phi_{2,zz} + \gamma\kappa\Phi_{1,z} - \gamma\Phi_{0,ss} - \gamma z\kappa^2\Phi_{0,z}.
\end{aligned}
\tag{71}
$$

This motivates the following definition of inner solutions.

Definition 5.2 (Inner solution and matching solution)**.** A tuple $(\Lambda_0, \mathbf{V}_0, \Phi_0, \Lambda_1, \Phi_1, \Lambda_2, \Phi_2)$ such that

$$
\begin{aligned}
\Lambda_0 &\in \mathrm{C}^0([0,T), \mathrm{C}^0(I, \mathrm{C}^2(\mathbb{R}))) \cap \mathrm{C}^0([0,T), \mathrm{C}^2(I, \mathrm{C}^0(\mathbb{R}))),\\
\Lambda_1, \Lambda_2, \Phi_2 &\in \mathrm{C}^0([0,T)\times I, \mathrm{C}^2(\mathbb{R})),\\
\Phi_0 &\in \mathrm{C}^0([0,T)\times I, \mathrm{C}^3(\mathbb{R})) \cap \mathrm{C}^0([0,T), \mathrm{C}^1(I, \mathrm{C}^2(\mathbb{R}))) \cap \mathrm{C}^0([0,T), \mathrm{C}^2(I, \mathrm{C}^0(\mathbb{R}))),\\
\Phi_1 &\in \mathrm{C}^0([0,T)\times I, \mathrm{C}^3(\mathbb{R})),\\
\mathbf{V}_0 &\in \mathrm{C}^0([0,T)\times I, \mathrm{C}^2(\mathbb{R}, \mathbb{R}^2)),
\end{aligned}
$$

is called an **inner solution of the strong capillarity regime**, provided it satisfies (65)-(70) and $\Phi_0 \not\equiv \frac{c_+}{c_-}$, where P_0, P_1, M_0, M_1 and M_2 are given by (71).

A tuple $(\lambda_0, \mathbf{v}_0, \varphi_0, \lambda_1, \varphi_1, \Lambda_0, \mathbf{V}_0, \Phi_0, \Lambda_1, \Phi_1, \Lambda_2, \Phi_2)$ is called a **matching solution of the strong capillarity regime**, if $(\lambda_0, \mathbf{v}_0, \varphi_0, \lambda_1, \varphi_1)$ is an inner and $(\Lambda_0, \mathbf{V}_0, \Phi_0, \Lambda_1, \Phi_1, \Lambda_2, \Phi_2)$ is an outer solution of the strong capillarity regime and both are linked by the matching conditions (45)-(53).

Theorem 5.3. *Let $(\lambda_0, \mathbf{v}_0, \varphi_0, \lambda_1, \varphi_1, \Lambda_0, \mathbf{V}_0, \Phi_0, \Lambda_1, \Phi_1, \Lambda_2, \Phi_2)$ be a matching solution of the strong capillarity regime. Then, $\varphi_0 = 1$ in $\Omega^+(t)$ for all $t \in [0,T)$ and $\varphi_0 = -1$ in $\Omega^-(t)$ for all $t \in [0,T)$, while λ_0 is constant in space in the whole domain. Moreover, in the bulk domains $\Omega^\pm(t)$ the fields satisfy*

$$
\operatorname{div}(\mathbf{v}_0) = 0, \quad \Delta(c_+W''(\varphi_0)\varphi_1 + c_-\lambda_1) = 0, \quad \nabla(p'(\varphi_0)\varphi_1 + \lambda_1) = 0. \tag{72}
$$

At the interface Γ *they are subject to the following jump conditions*

$$[\![\mathbf{v}_0 \cdot \mathbf{t}]\!] = 0, \qquad [\![c_+ W''(\varphi_0)\varphi_1 + c_-\lambda_1]\!] = 0, \qquad [\![\mathbf{v}_0 \cdot \boldsymbol{\nu}]\!] = \frac{c_- m_J}{2}[\![\nabla(c_+ W''(\varphi_0)\varphi_1 + c_-\lambda_1)]\!] \cdot \boldsymbol{\nu}, \tag{73}$$

$$[\![W''(\varphi_0)\varphi_1]\!] = \int_{-\infty}^{\infty} \frac{((\eta(\Phi_0) + 2\hat{\eta}(\Phi_0))(\mathbf{V}_0 \cdot \boldsymbol{\nu})_z)_z}{\Phi_0 - \frac{c_+}{c_-}}\,\mathrm{d}z, \qquad [\![p'(\varphi_0)\varphi_1 + \lambda_1]\!] = \kappa \int_{-\infty}^{\infty} (\Phi_{0,z})^2\,\mathrm{d}z, \tag{74}$$

and the normal velocity of the interface is given by

$$w_\nu = \langle \mathbf{v}_0 \cdot \boldsymbol{\nu} \rangle - \frac{c_+ m_J}{2}[\![\nabla(c_+ W''(\varphi_0)\varphi_1 + c_-\lambda_1)]\!] \cdot \boldsymbol{\nu}, \tag{75}$$

where $\langle \mathbf{v}_0 \cdot \boldsymbol{\nu} \rangle$ *denotes the mean value* $\frac{1}{2}(\mathbf{v}^+ \cdot \boldsymbol{\nu} + \mathbf{v}^- \cdot \boldsymbol{\nu})$*. Furthermore, the mean curvature of the interface has to be constant with respect to the interface parameter* s*.*

Remark 5.4. Let us also consider the momentum equation of order ε^{-1}. Abbreviating $p'(\varphi_0)\varphi_2 + \frac{1}{2}p''(\varphi_0)\varphi_1^2$, by p_2, we obtain from the outer expansions and the fact that φ_0 is constant the equation:

$$\rho(\varphi_0)(\mathbf{v}_{0,t} + (\mathbf{v}_0 \cdot \nabla)\mathbf{v}_0) + \nabla(p_2 + \lambda_2) = \operatorname{div}((\boldsymbol{\sigma}_{NS})_0) \quad \text{in } [0,T) \times \Omega^{\pm}(t). \tag{76}$$

Here, $(\boldsymbol{\sigma}_{NS})_0$ denotes the leading order of $\boldsymbol{\sigma}_{NS}$, where we have substituted $\varphi, \mathbf{v}$ by $\varphi_0, \mathbf{v}_0$. Thus, one has to solve incompressible Navier–Stokes equations in the bulk, where $(p_2 + \lambda_2)$ takes the role of the pressure. However, one cannot get the classical Young–Laplace law, as the surface tension is so strong in this case that it enforces the Young–Laplace law for $p_1 + \lambda_1$. If one considers the appropriate inner equations, one obtains – after rather cumbersome calculations –

$$\begin{aligned}[\![\rho(\varphi_0)(\mathbf{v}_0 \cdot \boldsymbol{\nu} - w_\nu)^2 + p_2 + \lambda_2 - \boldsymbol{\sigma}_{NS}^{ij}\nu^i\nu^j]\!] = -2\kappa \int_{-\infty}^{\infty} \hat{\eta}(\Phi_0)\mathbf{V}_{0,z} \cdot \boldsymbol{\nu}\,\mathrm{d}z + 2\gamma\kappa \int_{-\infty}^{\infty} \Phi_{0,z}\Phi_{1,z}\,\mathrm{d}z \\ - \gamma C_{ss}\int_{-\infty}^{\infty} (\Phi_{0,z})^2\,\mathrm{d}z + \gamma\kappa^2 C \int_{-\infty}^{\infty} (\Phi_{0,z})^2\,\mathrm{d}z.\end{aligned} \tag{77}$$

Here, C is a function, depending on τ and s, which appears as a translation term in the argument of Φ_0 compared with the reference solution $\bar{\Phi}_0$ satisfying $\bar{\Phi}_0(0) = 0$, cf. (102).

Proof of Theorem 5.3. As the proof is quite long, we decompose it into several parts.

Part 1: Firstly, we prove that $\varphi_0 = 1$ in $\Omega^+(t)$ for all $t \in [0,T)$ and $\varphi_0 = -1$ in $\Omega^-(t)$ for all $t \in [0,T)$. Secondly, we verify that λ_0 is constant in space in the whole domain.

We start by dividing (65) by c_- and subtracting (66), which gives because of (4) and (51)

$$\frac{c_+}{c_-}W''(\Phi_0)\Phi_{0,z} - \Phi_0 W''(\Phi_0)\Phi_{0,z} = \gamma\frac{c_+}{c_-}\Phi_{0,zzz} - \gamma\Phi_0\Phi_{0,zzz}. \tag{78}$$

For $\Phi_0 \neq \frac{c_+}{c_-}$, it follows

$$W''(\Phi_0)\Phi_{0,z} = \gamma\Phi_{0,zzz}. \tag{79}$$

Now, since $\Phi_0 \in C^0([0,T) \times I, C^3(\mathbb{R}))$, we may conclude by a continuity argument that (79) is equivalent to (78). This implies, using (45),

$$[\![W'(\varphi_0)]\!] = 0. \tag{80}$$

Integrating (79) and multiplying it by $\Phi_{0,z}$, we obtain

$$\begin{aligned} W'(\Phi_0)\Phi_{0,z} &= \gamma\Phi_{0,z}\Phi_{0,zz} + W'(\varphi_0^\pm)\Phi_{0,z} \\ \Longrightarrow [\![W(\varphi_0)]\!] &= \underbrace{\frac{1}{2}\int_{-\infty}^{\infty}((\Phi_{0,z})^2)_z \,\mathrm{d}z}_{=0} + W'(\varphi_0^\pm)[\![\varphi_0]\!]. \end{aligned} \tag{81}$$

From (81) we learn that $\varphi_0^\pm$ are the Maxwell points of W, cf. (7) for the definition. Due to our choice of W, this means

$$\varphi_0^\pm = \pm 1. \tag{82}$$

We know from (58) that $p(\varphi_0) + \lambda_0$ is constant in the bulk phases. Furthermore, we get from (66)

$$[\![p(\varphi_0) + \lambda_0]\!] = \int_{-\infty}^{\infty} \left(\Phi_0\Phi_{0,zz} - \frac{1}{2}\Phi_{0,z}^2\right)_z \mathrm{d}z = 0. \tag{83}$$

Hence, there is some time dependent function $K = K(t)$, such that

$$p(\varphi_0) + \lambda_0 = K(t) \tag{84}$$

in the bulk phases. Moreover, we know by integrating (65) that

$$[\![c_+ W'(\varphi_0) + c_-\lambda_0]\!] = 0. \tag{85}$$

Because of (58), (59), (64) and (82) the function $f_0 := c_+W'(\varphi_0) - c_-p(\varphi_0)$ satisfies the following problem in $\Omega^+(t)$ (and a similar problem in $\Omega^-(t)$):

$$\Delta f_0 = 0 \text{ in } \Omega^+(t), \quad \nabla f_0 \cdot \boldsymbol{\nu} = 0 \text{ on } \partial\Omega \cap \Omega^+(t), \quad f_0 = 0 \text{ on } \Gamma. \tag{86}$$

Problem (86) is uniquely solvable and the obvious solution is

$$0 = f_0 = c_+W'(\varphi_0) - c_-p(\varphi_0). \tag{87}$$

Due to the assumption (3) on the double well potential, this yields

$$\varphi_0 = \pm 1 \qquad \text{in } \Omega^\pm(t). \tag{88}$$

Finally, we combine (84) and (88) to see that λ_0 is constant in space in the whole domain.

Part 2: We show that $\operatorname{div}(\mathbf{v}_0) = 0$ and $\Delta(c_+W''(\varphi_0)\varphi_1 + c_-\lambda_1) = 0$ hold in the bulk phases $\Omega^\pm(t)$. Then, we prove the jump condition $[\![c_+W''(\varphi_0)\varphi_1 + c_-\lambda_1]\!] = 0$ on $\Gamma(t)$.

Combining (61) and (62), we get

$$\varphi_{0,t} + \nabla\varphi_0 \cdot \mathbf{v}_0 + \varphi_0 \operatorname{div}(\mathbf{v}_0) = \frac{c_+}{c_-}\operatorname{div}(\mathbf{v}_0). \tag{89}$$

In view of (88), this means

$$\underbrace{\left(\frac{c_+}{c_-} - \varphi_0\right)}_{>0} \operatorname{div}(\mathbf{v}_0) = 0 \Longrightarrow \operatorname{div}(\mathbf{v}_0) = 0. \tag{90}$$

Furthermore,by plugging (90) into (62), we find

$$\Delta(c_+W''(\varphi_0)\varphi_1 + c_-\lambda_1) = 0. \tag{91}$$

We continue by considering the inner equations. By (50) and (65) equation (67) becomes

$$(c_+M_1 + c_-\Lambda_1)_{zz} = 0.$$

This implies, using the matching condition (50), $\nabla\varphi_0 = 0$ and $\nabla\lambda_0 = 0$

$$(c_+M_1 + c_-\Lambda_1)_z = \left(\nabla\left(c_+W'(\varphi_0) + c_-\lambda_0\right)\right)^{\pm} \cdot \boldsymbol{\nu} = 0. \tag{92}$$

Thus, because of (46), we get

$$c_+M_1 + c_-\Lambda_1 = c_+W''(\varphi_0^{\pm})\varphi_1^{\pm} + c_-\lambda_1^{\pm}, \tag{93}$$

which directly implies

$$[\![c_+W''(\varphi_0)\varphi_1 + c_-\lambda_1]\!] = 0. \tag{94}$$

Part 3: We show the jump conditions $[\![\mathbf{v}_0\cdot\mathbf{t}]\!] = 0$ and $[\![p'(\varphi_0)\varphi_1+\lambda_1]\!] = \kappa\int_{-\infty}^{\infty}(\Phi_{0,z})^2\,\mathrm{d}z$ on $\Gamma(t)$. Furthermore, we conclude that the mean curvature κ is constant in space.

Due to (60), we find numbers $K^{\pm}(t)$, only depending on time, such that

$$p'(\varphi_0)\varphi_1 + \lambda_1 = K^{\pm}(t) \quad \text{in } \Omega^{\pm}(t). \tag{95}$$

Now, let us consider (68) to determine the jump of the first order expression for the pressure plus the Lagrange multiplier, i. e. $p'(\varphi_0)\varphi_1 + \lambda_1$, at the interface. Decomposing (68) into normal and tangential part, we obtain

$$(p'(\Phi_0)\Phi_1 + \Lambda_1)_z = (\bar\eta(\Phi_0)(\mathbf{V}_0\cdot\boldsymbol{\nu})_z)_z + \gamma(\Phi_1\Phi_{0,zzz} + \Phi_0\Phi_{1,zzz} - \kappa\Phi_0\Phi_{0,zz}), \tag{96}$$

$$(p(\Phi_0) + \Lambda_0)_s = (\hat\eta(\Phi_0)(\mathbf{V}_0\cdot\frac{\mathbf{t}}{\|\mathbf{t}\|^2})_z)_z\|\mathbf{t}\|^2 + \gamma\Phi_0\Phi_{0,zzs}, \tag{97}$$

where we abbreviate $\bar\eta(\Phi_0) = \eta(\Phi_0) + 2\hat\eta(\Phi_0)$. Let us first deal with (97). We already know from (66)

$$p(\Phi_0) + \Lambda_0 = \gamma\Phi_0\Phi_{0,zz} - \frac{\gamma}{2}(\Phi_{0,z})^2 + p(\varphi_0^{\pm}) + \lambda_0^{\pm}, \tag{98}$$

where $p(\varphi_0^{\pm}) + \lambda_0^{\pm}$ is independent of s. Plugging (66) into (97), we find

$$\gamma\left(\Phi_0\Phi_{0,zz} - \frac{1}{2}(\Phi_{0,z})^2\right)_s = (\hat\eta(\Phi_0)(\mathbf{V}_0\cdot\frac{\mathbf{t}}{\|\mathbf{t}\|^2})_z)_z\|\mathbf{t}\|^2 + \gamma\Phi_0\Phi_{0,zzs}, \tag{99}$$

which, in turn, implies

$$\gamma\Phi_{0,s}\Phi_{0,zz} - \gamma\Phi_{0,z}\Phi_{0,sz} = (\hat\eta(\Phi_0)(\mathbf{V}_0\cdot\frac{\mathbf{t}}{\|\mathbf{t}\|^2})_z)_z\|\mathbf{t}\|^2. \tag{100}$$

To understand the implications of (100), we have to investigate the s dependency of Φ_0 more carefully. We know that Φ_0 satisfies

$$W'(\Phi_0) = \gamma\Phi_{0,zz} + W'(\pm1) = \gamma\Phi_{0,zz}, \quad \Phi_0(\pm\infty) = \pm1. \tag{101}$$

As only the boundary data of Φ_0 and $\Phi_{0,z}$ are prescribed at infinity this does not determine Φ_0 uniquely, but we can write each solution as

$$\Phi_0(\tau, s, z) = \bar\Phi_0(z + C(\tau, s)) \tag{102}$$

where $\bar{\Phi}_0$ is the unique solution of (101) satisfying $\bar{\Phi}_0(0) = 0$ and C is a translational constant with respect to z. We like to mention that $\bar{\Phi}_0$ is a function of only one variable. Equation (102) has the following consequences for the partial derivatives of Φ_0 :

$$\Phi_{0,z}(\tau,s,z) = \bar{\Phi}_0'(z + C(\tau,s)), \qquad \Phi_{0,s}(\tau,s,z) = \bar{\Phi}_0'(z + C(\tau,s))C_s(\tau,s), \tag{103}$$

$$\Phi_{0,sz}(\tau,s,z) = \bar{\Phi}_0''(z + C(\tau,s))C_s(\tau,s), \qquad \Phi_{0,zz}(\tau,s,z) = \bar{\Phi}_0''(z + C(\tau,s)). \tag{104}$$

Hence,

$$\Phi_{0,s}(\tau,s,z)\Phi_{0,zz}(\tau,s,z) - \Phi_{0,z}(\tau,s,z)\Phi_{0,sz}(\tau,s,z) = 0. \tag{105}$$

We insert (105) into (100) and obtain because of the matching conditions

$$\hat{\eta}(\Phi_0)\mathbf{V}_{0,z} \cdot \mathbf{t} = 0. \tag{106}$$

As $\hat{\eta}(\Phi_0) \neq 0$, this implies

$$\mathbf{V}_{0,z} \cdot \mathbf{t} = 0 \tag{107}$$

and therefore

$$[\![\mathbf{v}_0 \cdot \mathbf{t}]\!] = 0. \tag{108}$$

We now turn to the normal part of the momentum balance, i.e. (96). We want to stress that because of (84) and (88) the matching conditions for Φ_1 and Λ_1 simplify to

$$\Phi_1(z) \to \varphi_1^{\pm},\ \Lambda_1(z) \to \lambda_1^{\pm}, \quad \text{for } z \to \pm\infty. \tag{109}$$

Because of (109), we get by integrating (96)

$$\begin{aligned}[\![p'(\varphi_0)\varphi_1 + \lambda_1]\!] &= [\bar{\eta}(\Phi_0)\mathbf{V}_{0,z} \cdot \boldsymbol{\nu} + \gamma(\Phi_{1,zz}\Phi_0 + \Phi_1\Phi_{0,zz} - \Phi_{0,z}\Phi_{1,z})]_{-\infty}^{+\infty} + \kappa\gamma\int_{-\infty}^{\infty}(\Phi_{0,z})^2\,\mathrm{d}z \\ &= \kappa\gamma\int_{-\infty}^{\infty}(\Phi_{0,z})^2\,\mathrm{d}z.\end{aligned} \tag{110}$$

We want to point out that due to (102) we have

$$\frac{\partial}{\partial s}\int_{-\infty}^{\infty}(\Phi_{0,z})^2\,\mathrm{d}z = 0. \tag{111}$$

Furthermore, it holds because of (95) that

$$\frac{\partial}{\partial s}[\![p'(\varphi_0)\varphi_1 + \lambda_1]\!] = 0. \tag{112}$$

Using (111) and (112) in (110), we find

$$\frac{\partial}{\partial s}\kappa = 0. \tag{113}$$

Part 4: We show that $[\![W''(\varphi_0)\varphi_1]\!] = \int_{-\infty}^{\infty} \frac{((\eta(\Phi_0)+2\hat{\eta}(\Phi_0))(\mathbf{V}_0\cdot\boldsymbol{\nu})_z)_z}{\Phi_0 - \frac{c_+}{c_-}}\,\mathrm{d}z$ on $\Gamma(t)$.

By combining (71),(92) and (96), we obtain

$$\begin{aligned}&\left(p'(\Phi_0)\Phi_1 - \frac{c_+}{c_-}W''(\Phi_0)\Phi_1 + \gamma\frac{c_+}{c_-}\Phi_{1,zz}\right)_z - \gamma\left(\Phi_1\Phi_{0,zzz} + \Phi_0\Phi_{1,zzz}\right) \\ &\qquad = (\bar{\eta}(\Phi_0)(\mathbf{V}_0 \cdot \boldsymbol{\nu})_z)_z - \gamma\kappa\Phi_0\Phi_{0,zz} + \gamma\frac{c_+}{c_-}\kappa\Phi_{0,zz}.\end{aligned} \tag{114}$$

Because of (79), this is equivalent to

$$\left(\Phi_0 - \frac{c_+}{c_-}\right)\left(W''(\Phi_0)\Phi_1 - \gamma\Phi_{1,zz}\right)_z = \left(\bar{\eta}(\Phi_0)(\mathbf{V}_0\cdot\boldsymbol{\nu})_z\right)_z - \gamma\kappa\Phi_0\Phi_{0,zz} + \gamma\frac{c_+}{c_-}\kappa\Phi_{0,zz}. \tag{115}$$

Due to $\nabla\varphi_0 = 0$, we can divide (115) by $\Phi_0 - \frac{c_+}{c_-}$ and integrate it, which yields

$$[\![W''(\varphi_0)\varphi_1]\!] = \int_{-\infty}^{\infty} \frac{\left((\eta(\Phi_0) + 2\hat{\eta}(\Phi_0))(\mathbf{V}_0\cdot\boldsymbol{\nu})_z\right)_z}{\Phi_0 - \frac{c_+}{c_-}}\,\mathrm{d}z.$$

Part 5: In this last part, we show the remaining jump condition $[\![\mathbf{v}_0\cdot\boldsymbol{\nu}]\!] = \frac{c_-m_J}{2}[\![\nabla(c_+W''(\varphi_0)\varphi_1 + c_-\lambda_1)]\!]\cdot\boldsymbol{\nu}$ on $\Gamma(t)$. Finally, we derive $w_\nu = \langle\mathbf{v}_0\cdot\boldsymbol{\nu}\rangle - \frac{c_+m_J}{2}[\![\nabla(c_+W''(\varphi_0)\varphi_1 + c_-\lambda_1)]\!]\cdot\boldsymbol{\nu}$, which completes the proof of the theorem.

Firstly, we observe that due to (92)

$$(c_+M_1 + c_-\Lambda_1)_z = 0.$$

Moreover, because of (65) together with the matching conditions and the fact that φ_0, λ_0 are constant in space, we get

$$(c_+M_0 + c_-\Lambda_0)_{ss} = 0.$$

Plugging the last two equations into (70), we obtain

$$(\mathbf{V}_0\cdot\boldsymbol{\nu})_z = c_-m_J(c_+M_2 + c_-\Lambda_2)_{zz}. \tag{116}$$

Because of $\nabla\varphi_0 = 0$ and $\nabla\lambda_0 = 0$ and the matching condition (53), we have

$$(c_+M_2 + c_-\Lambda_2)_{zz} \to 0 \quad \text{for } z \to \pm\infty$$

and integrating (116) gives

$$[\![\mathbf{v}_0\cdot\boldsymbol{\nu}]\!] = \frac{c_-m_J}{2}[\![\nabla(c_+W''(\varphi_0)\varphi_1 + c_-\lambda_1)]\!]\cdot\boldsymbol{\nu}. \tag{117}$$

Using the arguments leading to (116) again, we find

$$w_\nu\Phi_{0,z} = (\Phi_0\mathbf{V}_0\cdot\boldsymbol{\nu})_z - c_+m_J(c_+M_2 + c_-\Lambda_2)_{zz}. \tag{118}$$

By integrating (118), we get

$$w_\nu = \langle\mathbf{v}_0\cdot\boldsymbol{\nu}\rangle - \frac{c_+m_J}{2}[\![\nabla(c_+W''(\varphi_0)\varphi_1 + c_-\lambda_1)]\!]\cdot\boldsymbol{\nu}.$$

□

5.2. **Low Viscosity Scaling**

In this section, we will determine the sharp interface limit of the low viscosity scaling of our model given by (24)-(27) and (29). We will show that the resulting sharp interface model consists of the incompressible Euler equations in the bulk. At the interface we have a Young–Laplace law for the pressure.

Before we can state the results, we have to define outer, inner and matching solutions. The equations, which outer solutions have to satisfy, are obtained by inserting (36)-(38) into (24)-(27).

Definition 5.5 (Outer solution)**.** A tuple $(\lambda_0, \mathbf{v}_0, \varphi_0, \lambda_1, \varphi_1)$ such that

$$\begin{aligned}\lambda_0, \varphi_1, \lambda_1 &\in \mathrm{C}^0([0,T), \mathrm{C}^2(\bar{\Omega}^{\pm}(t), \mathbb{R})),\\ \varphi_0 &\in \mathrm{C}^1([0,T), \mathrm{C}^0(\bar{\Omega}^{\pm}(t), \mathbb{R})) \cap \mathrm{C}^0([0,T), \mathrm{C}^2(\bar{\Omega}^{\pm}(t), \mathbb{R})),\\ \mathbf{v}_0 &\in \mathrm{C}^0([0,T), \mathrm{C}^1(\bar{\Omega}^{\pm}(t), \mathbb{R}^2)) \cap \mathrm{C}^1([0,T), \mathrm{C}^0(\bar{\Omega}^{\pm}(t), \mathbb{R}^2)),\end{aligned}$$

with boundary data (64) is called an **outer solution of the low viscosity regime** provided it satisfies (58), (59), (61), (62) and

$$\rho(\varphi_0)(\mathbf{v}_{0,t} + (\mathbf{v}_0 \cdot \nabla)\mathbf{v}_0) + \nabla(p'(\varphi_0)\varphi_1 + \lambda_1) = 0, \tag{119}$$

where μ_0, μ_1 are given by (63) and $\varphi_0 \not\equiv \frac{c_+}{c_-}$. In addition, the boundary condition

$$\nabla\varphi_0 \cdot \boldsymbol{\nu} = 0 \text{ on } [0,T) \times \partial\Omega \tag{120}$$

has to be satisfied.

For the definition of inner solutions and matching solutions we insert (42)-(44) into (24)-(27) and change the partial derivatives according to (41). This leads to the following definition:

Definition 5.6 (Inner solution and matching solution)**.** A tuple $(\Lambda_0, \mathbf{V}_0, \Phi_0, \Lambda_1, \Phi_1, \Lambda_2, \Phi_2)$, such that

$$\begin{aligned}\Lambda_0 &\in \mathrm{C}^0([0,T), \mathrm{C}^0(I, \mathrm{C}^2(\mathbb{R}))) \cap \mathrm{C}^0([0,T), \mathrm{C}^2(I, \mathrm{C}^0(\mathbb{R}))),\\ \Lambda_1, \Lambda_2, \Phi_2 &\in \mathrm{C}^0([0,T) \times I, \mathrm{C}^2(\mathbb{R})),\\ \Phi_0 &\in \mathrm{C}^0([0,T) \times I, \mathrm{C}^3(\mathbb{R})) \cap \mathrm{C}^0([0,T), \mathrm{C}^1(I, \mathrm{C}^2(\mathbb{R}))) \cap \mathrm{C}^0([0,T), \mathrm{C}^2(I, \mathrm{C}^0(\mathbb{R}))),\\ \Phi_1 &\in \mathrm{C}^0([0,T) \times I, \mathrm{C}^3(\mathbb{R})),\\ \mathbf{V}_0 &\in \mathrm{C}^0([0,T) \times I, \mathrm{C}^2(\mathbb{R}, \mathbb{R}^2)).\end{aligned}$$

is called an **inner solution of the low viscosity regime**, provided it satisfies (65)-(67), (69), (70) and

$$\begin{aligned}&\rho(\Phi_0)(-w_\nu + \mathbf{V}_0 \cdot \boldsymbol{\nu})\mathbf{V}_{0,z} + (p'(\Phi_0)\Phi_1 + \Lambda_1)_z\boldsymbol{\nu} + (p(\Phi_0) + \Lambda_0)_s\frac{\mathbf{t}}{\|\mathbf{t}\|^2}\\ &= (\eta(\Phi_0) + 2\hat{\eta}(\Phi_0))(\mathbf{V}_0 \cdot \boldsymbol{\nu})_z)_z\boldsymbol{\nu} + (\hat{\eta}(\Phi_0)(\mathbf{V}_0 \cdot \mathbf{t})_z)_z\frac{\mathbf{t}}{\|\mathbf{t}\|^2} + \gamma(\Phi_0\Phi_{1,zzz} + \Phi_1\Phi_{0,zzz} - \kappa\Phi_0\Phi_{0,zz})\boldsymbol{\nu} + \gamma\Phi_0\Phi_{0,zzs}\frac{\mathbf{t}}{\|\mathbf{t}\|^2},\end{aligned} \tag{121}$$

where P_0, P_1, M_0, M_1, and M_2 are given by (71), and $\Phi_0 \not\equiv \frac{c_+}{c_-}$.

A tuple $(\lambda_0, \mathbf{v}_0, \varphi_0, \lambda_1, \varphi_1, \Lambda_0, \mathbf{V}_0, \Phi_0, \Lambda_1, \Phi_1, \Lambda_2, \Phi_2)$ is called a **matching solution of the low viscosity regime**, if $(\lambda_0, \mathbf{v}_0, \varphi_0, \lambda_1, \varphi_1)$ is an inner, $(\Lambda_0, \mathbf{V}_0, \Phi_0, \Lambda_1, \Phi_1, \Lambda_2, \Phi_2)$ is an outer solution of the low viscosity regime, both are linked by the matching conditions (45)-(53) and $\Phi_0 \not\equiv \frac{c_+}{c_-}$.

Theorem 5.7. *Let $(\lambda_0, \mathbf{v}_0, \varphi_0, \lambda_1, \varphi_1, \Lambda_0, \mathbf{V}_0, \Phi_0, \Lambda_1, \Phi_1, \Lambda_2, \Phi_2)$ be a matching solution of the low viscosity regime. Then, $\varphi_0 = 1$ in $\Omega^+(t)$ for all $t \in [0,T)$ and $\varphi_0 = -1$ in $\Omega^-(t)$ for all $t \in [0,T)$, while λ_0 is constant in space in the whole domain. Moreover, in the bulk domains, the fields satisfy*

$$\mathrm{div}(\mathbf{v}_0) = 0, \quad \Delta(c_+W''(\varphi_0)\varphi_1 + c_-\lambda_1) = 0, \quad \rho(\varphi_0)(\mathbf{v}_{0,t} + (\mathbf{v}_0 \cdot \nabla)\mathbf{v}_0) + \nabla(p'(\varphi_0)\varphi_1 + \lambda_1) = 0. \tag{122}$$

At the interface they are subject to the following jump conditions

$$[\![\mathbf{v}_0 \cdot \mathbf{t}]\!] = 0, \qquad [\![\mathbf{v}_0 \cdot \boldsymbol{\nu}]\!] = \frac{c_- m_J}{2}[\![\nabla(c_+ W''(\varphi_0)\varphi_1 + c_-\lambda_1)]\!] \cdot \boldsymbol{\nu}, \qquad [\![c_+ W''(\varphi_0)\varphi_1 + c_-\lambda_1]\!] = 0, \tag{123}$$

$$[\![W''(\varphi_0)\varphi_1]\!] = \frac{\hat{\rho}_2 - \hat{\rho}_1}{4} c_+ c_- j_0^2 + \int_{-\infty}^{\infty} \frac{((\eta(\Phi_0) + 2\hat{\eta}(\Phi_0))(\mathbf{V}_0 \cdot \boldsymbol{\nu})_z)_z}{\Phi_0 - \frac{c_+}{c_-}} \,\mathrm{d}z, \tag{124}$$

$$[\![\frac{j_0^2}{\rho(\varphi_0)} + p'(\varphi_0)\varphi_1 + \lambda_1]\!] = \kappa \int_{-\infty}^{\infty} (\Phi_{0,z})^2 \,\mathrm{d}z \tag{125}$$

where

$$j_0 := \rho(\varphi_0^{\pm})(\mathbf{v}_0^{\pm} \cdot \boldsymbol{\nu} - w_\nu)$$

is the mass flux across the interface, which is independent of the choice of $^+$ *or* $^-$*. Moreover, the normal velocity of the interface is given by*

$$w_\nu = \langle \mathbf{v}_0 \cdot \boldsymbol{\nu} \rangle - \frac{c_+ m_J}{2}[\![\nabla(c_+ W''(\varphi_0)\varphi_1 + c_-\lambda_1)]\!] \cdot \boldsymbol{\nu}. \tag{126}$$

As the equations satisfied by matching solutions of the low viscosity regime are very similar to those in case of the strong capillarity regime, we will not give a detailed proof of Theorem 5.7. We will only give a sketch of the differences between the proofs of Theorem 5.7 and Theorem 5.3.

Proof of Theorem 5.7. By the same arguments as in the proof of Theorem 5.3, we obtain

$$\begin{aligned} W''(\Phi_0)\Phi_{0,z} - \gamma\Phi_{0,zzz} = 0 \text{ in } [0,T) \times I \times \mathbb{R}, \qquad & \varphi_0 \mp 1 = 0 \text{ in } \Omega^{\pm}(t) \ \forall t \in [0,T), \\ \Lambda_0 = K(t) \text{ in } [0,T) \times I \times \mathbb{R}, \qquad & \lambda_0 = K(t) \text{ in } [0,T) \times \Omega^{\pm}, \\ c_+ M_1 + c_-\Lambda_1 - c_+ W''(\varphi_0^{\pm})\varphi_1^{\pm} - c_-\lambda_1^{\pm} = 0 \text{ in } [0,T) \times I \times \mathbb{R}, \qquad & \operatorname{div}(\mathbf{v}_0) = 0 \text{ in } [0,T) \times \Omega, \end{aligned}$$

and

$$\begin{aligned} [\![\mathbf{v}_0 \cdot \boldsymbol{\nu}]\!] &= \frac{c_- m_J}{2}[\![\nabla(c_+ W''(\varphi_0)\varphi_1 + c_-\lambda_1)]\!] \cdot \boldsymbol{\nu}, \\ w_\nu &= \langle \mathbf{v}_0 \cdot \boldsymbol{\nu} \rangle - \frac{c_+ m_J}{2}[\![\nabla(c_+ W''(\varphi_0)\varphi_1 + c_-\lambda_1)]\!] \cdot \boldsymbol{\nu}. \end{aligned}$$

Thus, the only equation we have to consider is (121), and it remains to show $(123)_1$,(124) and (125). The normal part of (121) reads

$$\begin{aligned} &\rho(\Phi_0)(\mathbf{V}_0 \cdot \boldsymbol{\nu} - w_\nu)(\mathbf{V}_0 \cdot \boldsymbol{\nu})_z + (p'(\Phi_0)\Phi_1 + \Lambda_1)_z \\ &\qquad = ((\eta(\Phi_0) + 2\hat{\eta}(\Phi_0))(\mathbf{V}_0 \cdot \boldsymbol{\nu})_z)_z + \gamma(\Phi_1\Phi_{0,zzz} + \Phi_0\Phi_{1,zzz} - \kappa\Phi_0\Phi_{0,zz}), \end{aligned} \tag{127}$$

while the tangential part is given by

$$\rho(\Phi_0)(\mathbf{V}_0 \cdot \boldsymbol{\nu} - w_\nu)(\mathbf{V}_0 \cdot \mathbf{t})_z + (p(\Phi_0) + \Lambda_0)_s = (\hat{\eta}(\Phi_0)(\mathbf{V}_0 \cdot \frac{\mathbf{t}}{\|\mathbf{t}\|^2})_z)_z \|\mathbf{t}\|^2 + \gamma\Phi_0\Phi_{0,zzs}. \tag{128}$$

Before we continue, it is important to note that by (69) and (70) we have

$$(\mathbf{V}_0 \cdot \boldsymbol{\nu} - w_\nu)\Phi_{0,z} = \left(\frac{c_+}{c_-} - \Phi_0\right)(\mathbf{V}_0 \cdot \boldsymbol{\nu})_z$$

which, using elementary algebra and (1),(8), implies that the mass flux over the interface fulfills

$$(J_0)_z = (\rho(\Phi_0)(\mathbf{V}_0 \cdot \boldsymbol{\nu} - w_\nu))_z = 0. \tag{129}$$

Thus, integration of (127) yields

$$[\![\rho(\varphi_0)(\mathbf{v}_0\cdot\boldsymbol{\nu}-w_\nu)\mathbf{v}_0\cdot\boldsymbol{\nu}+p'(\varphi_0)\varphi_1+\lambda_1]\!]=\kappa\gamma\int_{-\infty}^{\infty}(\Phi_{0,z})^2\,\mathrm{d}z,$$

which is equivalent to (125).

Equation (124) is proven analogously to the corresponding condition in Theorem 5.3. It is important to note that due to

$$\frac{c_+}{c_-}-\Phi_0=\frac{2}{\hat\rho_2-\hat\rho_1}\rho(\Phi_0)$$

the term

$$\frac{\rho(\Phi_0)(\mathbf{V}_0\cdot\boldsymbol{\nu}-w_\nu)(\mathbf{V}_0\cdot\boldsymbol{\nu})_z}{\frac{c_+}{c_-}-\Phi_0}=\frac{\hat\rho_2-\hat\rho_1}{2}(\mathbf{V}_0\cdot\boldsymbol{\nu}-w_\nu)(\mathbf{V}_0\cdot\boldsymbol{\nu}-w_\nu)_z$$

is integrable.

Now, we turn to the tangential part of the velocity. As Φ_0 is uniquely determined up to a translation term in its argument by the Maxwell construction and (66), we find as in the proof of Theorem 5.3

$$(p(\Phi_0)+\Lambda_0)_s=\gamma\Phi_0\Phi_{0,szz}.$$

Using this and (129), equation (128) can be simplified and we get

$$J_0\,(\mathbf{V}_0\cdot\mathbf{t})_z=(\hat\eta(\Phi_0)(\mathbf{V}_0\cdot\frac{\mathbf{t}}{\|\mathbf{t}\|^2})_z)_z\|\mathbf{t}\|^2. \tag{130}$$

There are two cases to distinguish: In case $J_0\neq 0$, integrating (130) gives $J_0[\![\mathbf{v}_0\cdot\mathbf{t}]\!]=0$. Otherwise, we have

$$0=(\hat\eta(\Phi_0)(\mathbf{V}_0\cdot\frac{\mathbf{t}}{\|\mathbf{t}\|^2})_z)_z\|\mathbf{t}\|^2, \tag{131}$$

which in view of the matching conditions and $\hat\eta(\Phi_0)>0$ also implies $[\![\mathbf{v}_0\cdot\mathbf{t}]\!]=0$. This finishes the proof of the theorem. □

6. Numerical Treatment

As a first step towards a numerical treatment of the system (9)-(12) we give a numerical scheme for the Cahn–Hilliard equation with advection. As the equation contains derivatives up to 4th order, the Local Discontinuous Galerkin (LDG) method is attractive, because the equation can be rewritten as a system of first order equations and therefore methods for first order equations can be applied. Besides the fact that the LDG method is rather easy to implement, this method is known to be suitable for problems with strong advection terms. Furthermore, DG methods easily allow the use of higher order discretization, grid adaptivity and parallelization. We have implemented the Discontinuous Galerkin method [25] and combined it with an advection term. The code for the numerical experiments is written in C++ using the libraries Dune and Dune–Fem.

6.1. The Local Discontinuous Galerkin Method

To see if the LDG method is suitable for the numerical treatment of the system (9)-(12), we consider, in a first step, the Cahn–Hilliard equation with advection which is similar to the evolution of the phase field variable, see (9) and (12),

$$\varphi_t+\operatorname{div}(\varphi\mathbf{v})-\Delta(-\gamma\Delta\varphi+W'(\varphi))=0 \tag{132}$$

with a given $\mathbf{v}:\Omega\to\mathbb{R}^n$.

By introducing auxiliary functions $\mathbf{Q}, \mathbf{P} : \Omega \to \mathbb{R}^n$ and $\sigma : \Omega \to \mathbb{R}$, equation (132) can be written as the following system of first order equations

$$\begin{aligned} \mathbf{Q} &= \nabla\varphi, && (133)\\ \sigma &= \gamma \operatorname{div} \mathbf{Q} - W'(\varphi), && (134)\\ \mathbf{P} &= \nabla(-\sigma), && (135)\\ \varphi_t &= -\operatorname{div}(\mathbf{F}(\varphi) - \mathbf{P}), && (136) \end{aligned}$$

where $\mathbf{F}(\varphi) := \mathbf{v}\varphi$ denotes the advective flux. To define the LDG scheme, we give some notations regarding the mesh and the ansatz spaces used for the discretization.

Definition 6.1. Let $\mathcal{T} = \{E\}$ be a partition of Ω into polygons E and let let $E^+, E^- \in \mathcal{T}$,share an edge $e := \partial E^+ \cap \partial E^-$. Furthermore, let ϕ be a function, which is smooth within E^+ and E^-, but might be discontinuous across e, then the inner and outer trace of ϕ on e with respect to E^+ is given by

$$\phi^+(\mathbf{x}) := \lim_{\epsilon \nearrow 0} \phi(\mathbf{x} + \epsilon \boldsymbol{\nu}_E^+), \quad \phi^-(\mathbf{x}) := \lim_{\epsilon \nearrow 0} \phi(\mathbf{x} + \epsilon \boldsymbol{\nu}_E^-).$$

Furthermore, if we choose for every egde e a unique normal $\boldsymbol{\nu}_e$ imposing an orientation for every edge, we can define the "left" and "right" traces by

$$\phi_L(\mathbf{x}) := \lim_{\epsilon \nearrow 0} \phi(\mathbf{x} + \epsilon \boldsymbol{\nu}_e), \quad \phi_R(\mathbf{x}) := \lim_{\epsilon \nearrow 0} \phi(\mathbf{x} + \epsilon \boldsymbol{\nu}_e).$$

We want to approximate the solution of the system (133)-(136) with piecewise polynomial functions. Therefore, we define the discrete function spaces

$$V_h = \{\mathbf{v} \in \mathrm{L}^2(\Omega, \mathbb{R}) : \mathbf{v}|_E \in \mathcal{P}_E\}, \quad \Sigma_h = V_h^d,$$

where $\mathcal{P}_E$ denotes the space of polynomials of order $\leq k$ on E.

Remark 6.2. As there are no continuity restrictions on the discrete functions across the edges, one can choose an elementwise orthonormal basis for V_h and Σ_h.

The numerical scheme is then derived by multiplying the equations (133)-(136) by test functions $\psi, \tau \in V_h$, $\mathbf{R}, \mathbf{S} \in \Sigma_h$ and integrating by parts on each element E. We get the following system, where the values on the element edges are approximated by so–called numerical fluxes $\widehat{\varphi}$, $\widehat{\mathbf{Q}}$, $\widehat{\sigma}$, $\widehat{\mathbf{P}}$ and $\widehat{\mathbf{F}}$ depending on the left and right traces of φ, $\mathbf{Q}$, σ, $\mathbf{P}$ and φ respectively:

$$\begin{aligned} \int_E \mathbf{Q} \cdot \mathbf{R} \,\mathrm{d}\mathbf{x} &= -\int_E \operatorname{div} \mathbf{R}\varphi \,\mathrm{d}\mathbf{x} + \sum_{e \subset \partial E} \int_e \widehat{\varphi}(\varphi_L, \varphi_R) \boldsymbol{\nu}_E \cdot \mathbf{R}^- \,\mathrm{d}s, && (137)\\ \int_E \sigma\psi \,\mathrm{d}\mathbf{x} &= -\int_E W'(\varphi)\psi \,\mathrm{d}\mathbf{x} - \int_E \gamma \nabla\psi \cdot \mathbf{Q} \,\mathrm{d}\mathbf{x} + \sum_{e \subset \partial E} \int_e \widehat{\mathbf{Q}}(\mathbf{Q}_L, \mathbf{Q}_R) \cdot \boldsymbol{\nu}_E \psi^- \,\mathrm{d}s, && (138)\\ \int_E \mathbf{P} \cdot \mathbf{S} \,\mathrm{d}\mathbf{x} &= -\int_E -\sigma \operatorname{div} \mathbf{S} \,\mathrm{d}\mathbf{x} + \sum_{e \subset \partial E} \int_e -\widehat{\sigma}(\sigma_L, \sigma_R) \boldsymbol{\nu}_E \cdot \mathbf{S}^- \,\mathrm{d}s, && (139)\\ \int_E \partial_t \varphi\tau \,\mathrm{d}\mathbf{x} &= -\int_E (\mathbf{F}(\varphi) + \mathbf{P}) \cdot \nabla\tau \,\mathrm{d}\mathbf{x} + \sum_{e \subset \partial E} \int_e \left(\widehat{\mathbf{F}}(\varphi_L, \varphi_R) + \widehat{\mathbf{P}}(\mathbf{P}_L, \mathbf{P}_R)\right) \cdot \boldsymbol{\nu}_E \tau^- \,\mathrm{d}s. && (140) \end{aligned}$$

Here, $\boldsymbol{\nu}_E$ denotes the outer normal with respect to the element E.

The numerical fluxes for the Cahn–Hilliard part on a given edge $e \subset \partial E$ are defined as

$$\widehat{\varphi}(\varphi_L, \varphi_R)|_e = \varphi_L, \quad \widehat{\mathbf{Q}}(\mathbf{Q}_L, \mathbf{Q}_R)|_e = \mathbf{Q}_R, \quad \widehat{\sigma}(\sigma_L, \sigma_R)|_e = \sigma_L, \quad \widehat{\mathbf{P}}(\mathbf{P}_L, \mathbf{P}_R|_e = \mathbf{P}_R,$$

if e is an interior edge, that is $e = \partial E^+ \cap \partial E^-$ for $E^+, E^- \in \mathcal{T}$ and

$$\widehat{\varphi}|_e = \varphi|_e, \quad \widehat{\mathbf{Q}}|_e = 0, \quad \widehat{\sigma}|_e = \sigma|_e, \quad \widehat{\mathbf{P}}|_e = 0$$

if $e = \partial E \cap \partial\Omega$.

For the advective numerical flux $\widehat{\mathbf{F}}(\varphi^+, \varphi^-)$, a wide range of different numerical fluxes for finite volume schemes like the Lax–Friedrich flux or Riemann solvers, see e.g. [18], exist. In our case the velocity $\mathbf{v}$ is known, so we can apply a simple upwind flux.

Remark 6.3. This choice of numerical fluxes for the Cahn–Hilliard part leads to a L^2-stability result shown in [25]. As its proof relies on the fact that the values of $\widehat{\varphi}$ and $\widehat{\mathbf{Q}}$, $\widehat{\sigma}$ and $\widehat{\mathbf{P}}$, respectively, are taken from opposite sides, there are other possible choices for the fluxes.

Remark 6.4. When the full system (9)-(12) is treated, the velocity $\mathbf{v}$ is an unknown of the system and the advective flux will depend also on $\mathbf{v}$ so one has $\mathbf{F}(\mathbf{v}, \varphi)$ and $\widehat{\mathbf{F}}(\varphi^+, \mathbf{v}^+, \varphi^-, \mathbf{v}^-)$ in (140).

6.2. **Implementation**

We solve equations (137)-(140) for the intermediate variables $\mathbf{Q}, \sigma, \mathbf{P}$ and for φ_t by inverting the mass matrix on the left hand side. Written in operator form we have:

$$\mathbf{Q} = L_1[\varphi], \quad \sigma = L_2[\mathbf{Q}, \varphi], \quad \mathbf{P} = L_3[\sigma], \quad \varphi_t = L_4[\mathbf{P}, \varphi].$$

As the support of each base function is contained in one element and the base functions are L^2-orthogonal, the mass matrix can be inverted elementwise by dividing by the volume of the respective element. So the application of each of the operators L_1 to L_4 can be realized in one iteration over the triangulation. We finally have to solve a system of ordinary differential equations:

$$\varphi_t = L_4[L_3[L_2[L_1[\varphi], \varphi]], \varphi].$$

For solving the systems of ODEs arising in LDG methods, a common choice is to use explicit or implicit Runge-Kutta methods of higher order, see [10] and the references therein.

6.3. **Numerical Examples**

6.3.1. *Example in 1d*

To verify the convergence of our implementation, we compare the evolution of an initial profile with an exact equilibrium solution. We take the following double well and zero velocity

$$W(\varphi) = \frac{1}{4}(1 - \varphi^2)^2, \quad \mathbf{v} = 0.$$

Then $\varphi_{eq}(x) = \tanh(\frac{x}{\sqrt{2\gamma}})$ is an equilibrium solution of (132). We start with an initial data φ_0 close to φ_{eq}, i.e. $\varphi_0(x) = 0.8 \tanh(\frac{x}{\sqrt{2\gamma}})$. We run the simulation until the difference between two time steps in the L^2–norm divided by the time step size is smaller than $1e-10$. We observe that the equilibrium solution is approximated with the expected order, see Table 1.

6.3.2. *Example in 2d without convection*

In the first two dimensional example, the piecewise constant initial data on the domain $(0, 1)^2$ has the shape of an ellipse. The underlying mesh has 40×40 elements. We use $\mathcal{P}^1$ functions, periodic boundary conditions and $\gamma = 0.001$. We observe that the ellipse evolves into a sphere minimizing the length of the transition layer, see Fig. 1.

	$\mathcal{P}^1$		$\mathcal{P}^2$		$\mathcal{P}^3$	
h	L^2–error	EOC	L^2–error	EOC	L^2–error	EOC
0.05000	$2.81462e-2$	—	$9.44438e-3$	—	$5.79808e-3$	—
0.02500	$4.13528e-3$	2.76688	$2.72828e-3$	1.79146	$4.99597e-4$	3.53674
0.01250	$1.03695e-3$	1.99563	$3.07464e-4$	3.14950	$2.54611e-5$	4.29440
0.00625	$2.59519e-4$	1.99844	$3.91388e-5$	2.97375	$1.58700e-6$	4.00392

TABLE 1. Error and EOC for the 1d test case.

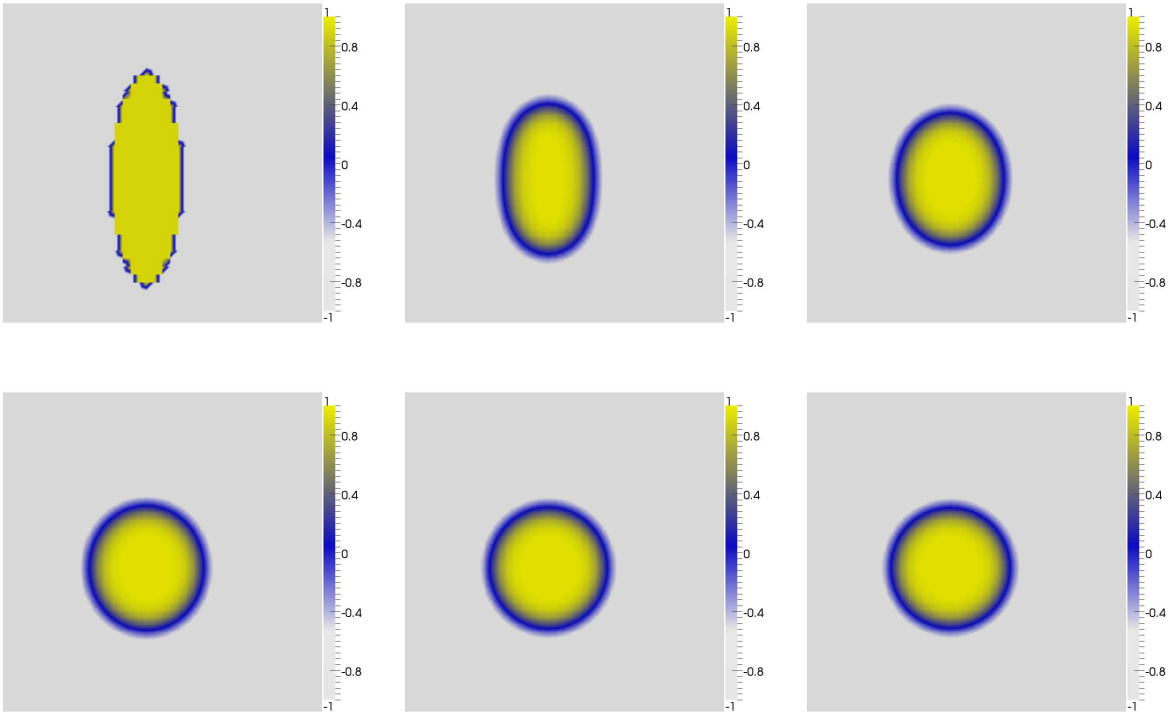

FIGURE 1. Evolution of an ellipse at time $0.0, 0.05, 0.10, 0.15, 0.20, 0.25$

6.3.3. *Example in 2d with convection*

In the second example, we introduce a velocity field $\mathbf{v}$ to the same initial data φ_0 as in the previous example. We set $\mathbf{v} = (0, 2x_1(x_1 - 1))^T$. Again the domain is $(0, 1)^2$, discretized by a 40×40 mesh, and γ is set to 0.001. The results show that the ellipse rapidly evolves to a sphere and is then transported by the velocity field, see Fig. 2. This shows that the LDG method is capable of solving the Cahn–Hilliard equation even if strong convection is present.

6.4. **Summary**

The LDG method from [25] combined with an upwind flux for the advection term was shown to be capable of approximating the Cahn–Hilliard equation with additional advection. The code used for the simulations can be run in parallel and can easily be extended with local mesh refinement. However, one has to mention that this approach suffers some drawbacks. We observed a severe time step restriction due to the higher order derivatives.

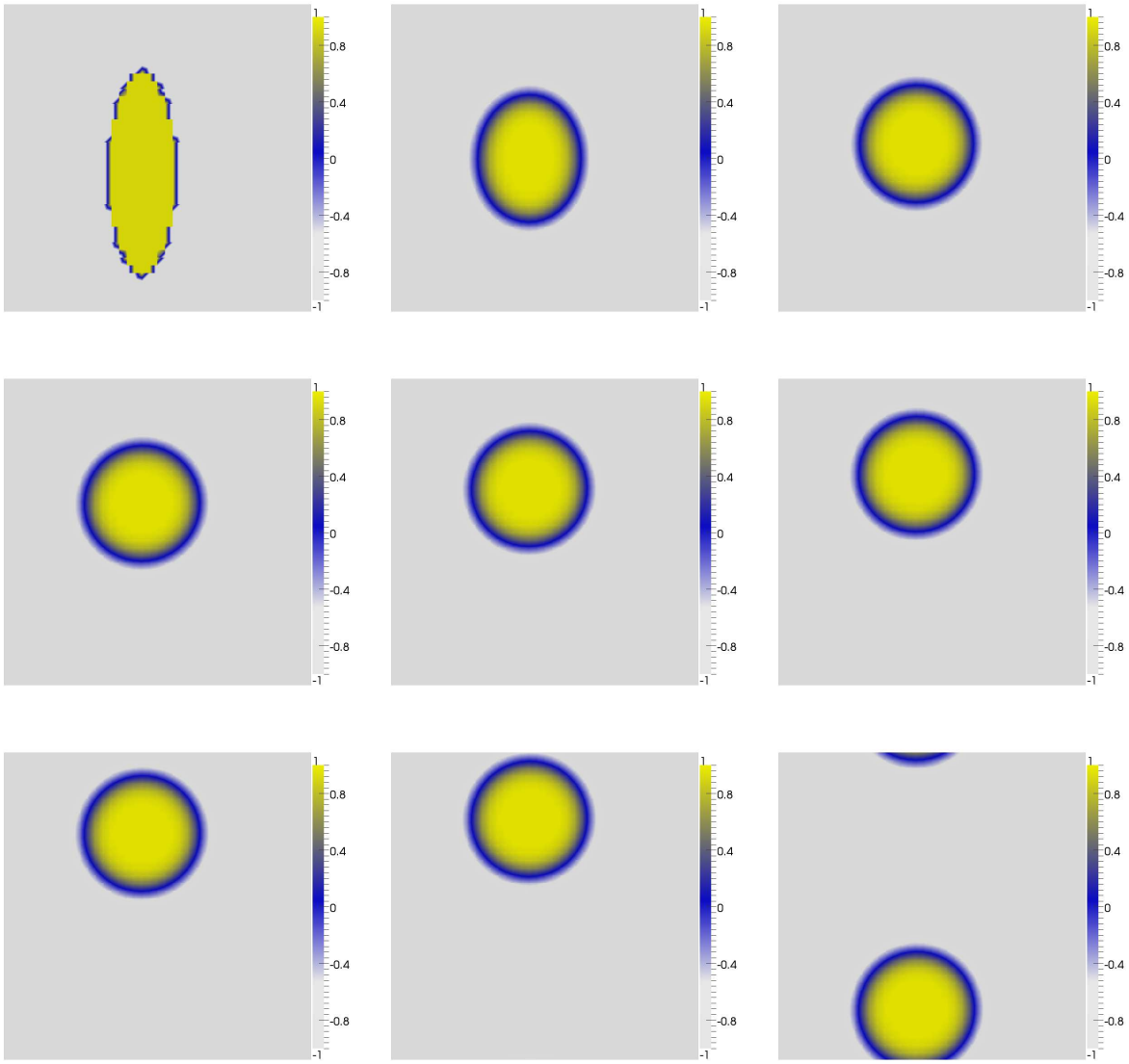

FIGURE 2. Evolution of an ellipse at time $t = 0.0, 0.1, ..., 0.7$ and end time $t = 1.5$

To achieve stability of the computations a time step restriction of the form $\Delta t \leq C\Delta x^4$ was required. On the one hand, this time step restriction is not as bad as it seems, because $C \sim \gamma^{-1}$ and in practice one will use $\Delta x \sim \gamma^{-1/2}$. On the other hand, for this choice the time step restriction is still $\Delta t \leq C\Delta x^2$ with $C = \mathcal{O}(1)$, which renders explicit time stepping too expensive. For this reason, we used an implicit scheme for the numerical examples. Having said that, the currently implemented matrix-free implicit scheme has the disadvantage that preconditioning is not easy to implement. So, we have to choose a small time step, even in the implicit case to guarantee the convergence of the inner linear solver. As every iteration of the solver needs the evaluation of the full operator, the overall computational costs in some cases may become similar to those of an explicit scheme with a much smaller time step. To overcome this problem one can implement the actual Jacobi matrix of the discrete operator. This will enable the use of standard preconditioning techniques and in each iteration

only one matrix-vector multiplication will be needed in comparison to four grid iterations. The assembling of the Jacobian is not easy because the LDG scheme leads to a large number of matrix entries in the case of 4th order derivatives. Therefore, the so–called CDG method presented in [22], which leads to a simpler and more sparse matrix structure, could be a way to overcome these difficulties.

References

[1] H. Abels. Diffuse interface models for two–phase flows of viscous incompressible fluids, 2007. Lecture Notes, Max Planck Institute for Mathematics in the Sciences, No. 36/2007.

[2] H. Abels, H. Garcke, and G. Grün. Thermodynamically consistent, frame indifferent diffuse interface models for incompressible two–phase flows with different densities, http://www.citebase.org/abstract?id=oai:arXiv.org:1104.1336, 2011.

[3] R. Abeyaratne and J. K. Knowles. Kinetic relations and the propagation of phase boundaries in solids. *Arch. Rational Mech. Anal.*, 114(2):119–154, 1991.

[4] G. L. Aki, W. Dreyer, J. Giesselmann, and C. Kraus. An incompressible diffuse model with phase transition. in preparation.

[5] H. W. Alt. The entropy principle for interfaces. Fluids and solids. *Adv. Math. Sci. Appl.*, 19(2):585–663, 2009.

[6] D. M. Anderson, G. B. McFadden, and A. A. Wheeler. Diffuse–interface methods in fluid mechanics. In *Annual review of fluid mechanics, Vol. 30*, pages 139–165. 1998.

[7] F. Boyer. A theoretical and numerical model for the study of incompressible mixture flows. *Computers and Fluids*, 31(1):41–68, 2002.

[8] G. Caginalp and P. C. Fife. Dynamics of layered interfaces arising from phase boundaries. *SIAM J. Appl. Math.*, 48(3):506–518, 1988.

[9] J. W. Cahn and J. E. Hilliard. Free Energy of a Nonuniform System. I. Interfacial Free Energy. *J. Chem. Phys.*, 28(2):258–267, 1958.

[10] D Diehl. *Higher order schemes for simulation of compressible liquid–vapor flows with phase change*. PhD thesis, Universität Freiburg, 2007. http://www.freidok.uni-freiburg.de/volltexte/3762/.

[11] H. Ding, P.D.M. Spelt, and C. Shu. Diffuse interface model for incompressible two–phase flows with large density ratios. *J. Comp. Phys.*, 226(2):2078–2095, 2007.

[12] W. Dreyer, J. Giesselmann, C. Kraus, and C. Rohde. Asymptotic analysis for korteweg models. SimTech Preprint 2010-67, http://www.simtech.uni-stuttgart.de/publikationen/preprints10.php, to appear in Interfaces and Free Boundaries.

[13] W. Dreyer and C. Kraus. On the van der Waals–Cahn–Hilliard phase–field model and its equilibria conditions in the sharp interface limit. *Proc. R. Soc. Edinb., Sect. A, Math.*, 140(6):1161–1186, 2010.

[14] M. E. Gurtin, D. Polignone, and J. Viñals. Two–phase binary fluids and immiscible fluids described by an order parameter. *Math. Models Methods Appl. Sci.*, 6(6):815–831, 1996.

[15] K. Hermsdörfer, C. Kraus, and D. Kröner. Interface conditions for limits of the Navier–Stokes–Korteweg model. *Interfaces Free Bound.*, 13(2):239–254, 2011.

[16] P. C. Hohenberg and B. I. Halperin. Theory of dynamic critical phenomena. *Rev. Mod. Phys.*, 49:435–479, 1977.

[17] T. Y. Hou, J. S. Lowengrub, and M. J. Shelley. The long–time motion of vortex sheets with surface tension. *Phys. Fluids*, 9(7):1933–1954, 1997.

[18] D. Kröner. *Numerical Schemes for Conservation Laws*. Wiley & Teubner, 1997.

[19] P. G. LeFloch. *Hyperbolic systems of conservation laws. The theory of classical and nonclassical shock waves*. Lectures in Mathematics ETH Zürich. Birkhäuser Verlag, Basel, 2002.

[20] J. Lowengrub and L. Truskinovsky. Quasi–incompressible Cahn–Hilliard fluids and topological transitions. *R. Soc. Lond. Proc. Ser. A Math. Phys. Eng. Sci.*, 454(1978):2617–2654, 1998.

[21] N.C. Owen, J. Rubinstein, and P. Sternberg. Minimizers and gradient flows for singularly perturbed bi–stable potentials with a Dirichlet condition. *Proc. R. Soc. Lond., Ser. A*, 429(1877):505–532, 1990.

[22] J. Peraire and P.-O. Persson. The compact discontinuous Galerkin (CDG) method for elliptic problems. *SIAM J. Sci. Comput.*, 30(4):806–1824, 2008.

[23] P. Sternberg. The effect of a singular perturbation on nonconvex variational problems. *Arch. Ration. Mech. Anal.*, 101(3):209–260, 1988.

[24] J. D. Van der Waals. Thermodynamische theorie der kapillarität unter voraussetzung stetiger dichteänderung. *Z. Phys. Chem*, 13:657–725, 1894.

[25] Y. Xia, Y. Xu, and C.-W. Shu. Local discontinuous galerkin methods for the cahn–hilliard type equations. *J. Comput. Phys.*, 227:472–491, 2007.